Estimating the Fed's Unconventional Policy Shocks*

Marek Jarociński†

This version: November 3, 2022

Abstract

Fed monetary policy announcements convey a mix of news about different conventional and unconventional policies, and about the economy. Financial market responses to these announcements are usually very small, but sometimes very large. I estimate the underlying structural shocks exploiting this feature of the data, both assuming that the structural shocks are independent and relaxing this assumption. Either approach yields the same tightly estimated shocks that can be naturally labeled as standard monetary policy, Odyssean forward guidance, large scale asset purchases and Delphic forward guidance.

JEL classification: E52, E58, E44

Keywords: High-frequency identification, Non-Gaussianity, Fat tails, Forward guidance, Asset purchases

*The opinions in this paper are those of the author and do not necessarily reflect the views of the European Central Bank or the New York Fed. I thank for comments an anonymous referee of the ECB working paper series, Jesús Fernández-Villaverde, Michael Johannes, Peter Karadi, Giorgio Primiceri and numerous seminar and conference participants.

†European Central Bank DG-Research (on secondment at the New York Fed), email: marek.jarocinski@gmail.com.

1 Introduction

Modern central banks deploy a variety of policies in their efforts to steer the economy and measuring the effects of these different policies is of paramount importance for monetary economics. Since Kuttner (2001), many papers identify monetary policy shocks from the changes of financial asset prices in a narrow time window around Federal Open Market Committee (FOMC) announcements. Prior to the announcement, asset prices reflect the consensus view on the state of the economy and the Fed's expected response to it. Afterwards, asset prices incorporate also any unexpected news conveyed in the announcement. These news could be about the current fed funds rate or its future path, asset purchases, the Fed's view on the state of the economy, etc. They represent different structural shocks that may affect the economy differently, so it is crucial to disentangle their effects.

This paper estimates the structural shocks that underlie the financial market reactions to FOMC announcements. While the nature of the shocks is not specified ex ante, ex post the estimated shocks can be naturally labeled as the current fed funds rate policy, an "Odyssean" forward guidance (a commitment to a future course of policy rates), a large scale asset purchase and a "Delphic" forward guidance (a statement about the future course of policy rates understood as a forecast of the appropriate stance of the policy rather than a commitment, see Campbell et al. 2012).

To estimate the structural shocks I exploit a striking, yet hitherto neglected feature of the data. Namely, the reactions of financial variables, such as interest rates and stock prices, to FOMC announcements are usually very small, but sometimes very large, i.e. they have very fat tails, or excess kurtosis. This feature implies that these data may contain information about the nature of the underlying structural shocks. Given the importance of the Fed policies, it is vital to exploit this available information as well as possible. Previous literature has ignored it, treating the shocks explicitly or implicitly as Gaussian. This paper is, to my knowledge, the first attempt to tap this valuable source of information.

Intuitively, fat-tailed shocks can be identified from the data because they tend to produce informative case studies. When we see a significant market reaction to an FOMC announcement, and the underlying shocks are independent and fat-tailed, there is a high

chance that only a subset of the shocks is driving this reaction, while the others are very small. This greatly facilitates detecting the unique patterns in the data corresponding to individual shocks. As a result, the shocks are identifiable from the data via the likelihood function alone, even in the absence of economic identifying restrictions. One contribution of this paper is to provide the intuition of the identification based on fat tails using a simple supply and demand example. The example also illustrates how identification weakens, and eventually vanishes, when the independence assumption is relaxed, which is particularly relevant in the case of disentangling Fed policies.

It is a separate question why the Fed shocks' reflections in financial data are fat tailed. One reason could be that the Fed generally avoids surprising financial markets, until occasionally it is forced to do it big time. Another reason could be that investors process information imperfectly and focus only on the most salient dimensions (Van Nieuwerburgh and Veldkamp, 2010).

My baseline model expresses the surprises (i.e., the high-frequency reactions to FOMC announcements) in the near-term fed funds futures, 2- and 10-year Treasury yield and the S&P500 stock index as linear combinations of four Student-t distributed shocks. It turns out that these four shocks are very precisely estimated and ex post have natural economic interpretations. The first shock raises the near-term fed funds futures, with a diminishing effect on longer maturities, and depresses the stock prices. It can be naturally labeled as the standard monetary policy shock. The second shock increases the 2-year Treasury yield the most and depresses the stock prices. It can be naturally labeled as the (Odyssean) forward guidance shock. The third shock increases the 10-year Treasury yield the most and plays a large role in some of the most important asset purchase announcements. It can be naturally labeled as the asset purchase shock. The fourth shock has a similar impact on the yield curve as the Odyssean forward guidance shock, but triggers an increase, rather than a decrease, in the stock prices. Therefore, this shock matches the concept of Delphic forward guidance introduced by Campbell et al. (2012). I find very similar four shocks when repeating the estimation on the principal components of a larger dataset and under a variety of other modifications of the baseline model.

The findings of this paper are relevant for the ongoing research on the effectiveness of

non-standard monetary policies. I track the effects of the estimated shocks using daily local projections. I find persistent and significant effects of non-standard policies (Odyssean forward guidance and asset purchases) on long term Treasury yields. The shocks gradually propagate through the financial system and after a few days get reflected also in the corporate bond spreads. Also the Delphic forward guidance shocks have significant and persistent effects on financial variables and contribute to the historical narrative of Fed policies. One of the largest Delphic shocks occurs in August 2011, when the Fed stated that exceptionally low interest rates will be warranted at least through mid-2013, triggering pessimism about the economy.

It is important that the results are robust to relaxing the assumption that the structural shocks are independent. If different Fed shocks tend to be large simultaneously (e.g. if they have some common stochastic volatility), the identification from fat-tails gets diluted and eventually vanishes (e.g. Montiel Olea et al., 2022). To account for this possibility, I generalize the Independent Student-t model and allow endogenously determined dependence of the tail behavior. More in detail, I design a new Partially Dependent Multivariate t-distribution (PDMT), which nests the Independent t and Multivariate t as extreme cases and spans all intermediate degrees of tail dependence between these extremes. The PDMT model estimated with data augmentation methods (Jacquier et al., 2007) and applied to the Fed policy shocks detects some tail dependence, but there is also a sufficient degree of tail independence to yield tight identification and virtually the same estimated shocks.

Previous research has used a variety of approaches and assumptions to decompose the financial market reactions into economically interpretable components (see Gürkaynak et al., 2005; Inoue and Rossi, 2018; Cieślak and Schrimpf, 2019; Lewis, 2019; Swanson, 2021; Miranda-Agrippino and Ricco, 2021; Jarociński and Karadi, 2020, and others). Most of these papers ignore the non-Gaussianity in the data and construct the shocks with the a priori assumed features. They often use identifying restrictions familiar from the Structural VAR literature. For example, Gürkaynak et al. (2005) separate the target factor (standard monetary policy) from the path factor (forward guidance) imposing a *zero restriction* on the response of short term rates to forward guidance. Swanson (2021) imposes a *narrative restriction* that the asset purchase shock is small prior to the Zero Lower Bound (ZLB)

period. Jarociński and Karadi (2020) separate monetary policy (a summary of standard and non-standard policies) from information (Delphic) shocks using *sign restrictions*. It is very interesting that, although I do not impose any of these restrictions, the shocks I estimate satisfy them (sometimes up to a numerical approximation). They are also highly correlated with their counterparts in these papers. Thus, my approach provides a statistical validation of the assumptions imposed in these papers. That said, I refine these papers' interpretations of the data by distinguishing four main shocks, while they identify at most three.

Identification through non-Gaussianity, such as the excess kurtosis exploited here, has been known since the 1990s but economic applications have started to appear only recently. This source of identification underlies the Independent Components Analysis (ICA) (Comon, 1994; Hyvärinen et al., 2001), which is widely used in signal processing, telecommunications and medical imaging. Bonhomme and Robin (2009) use ICA to identify factor loadings. Methodologically closest paper to the present one is Lanne et al. (2017) who identify structural VARs with Student-t shocks. Gouriéroux et al. (2017) extend the inference on Structural VARs to pseudo-maximum likelihood. Gouriéroux et al. (2020) show that also the Structural Vector Autoregression Moving Average (SVARMA) model is identified under shock non-Gaussianity. Fiorentini and Sentana (2020) study the effects of distributional misspecification and identify a structural VAR of volatility indices. Drautzburg and Wright (2021) use non-Gaussianity to strengthen the identification in sign-restricted in VARs. Braun (2021) applies identification through non-Gaussianity to the oil market. Davis and Ng (2022) provide econometric theory for VARs with disaster-type shocks and apply it to economic uncertainty and Covid shocks.

There are analogies between identification by non-Gaussianity and identification by heteroskedasticity (Rigobon, 2003). Both approaches are examples of a statistical identification exploiting that the shocks arrive "irregularly". For some recent applications of identification by heteroskedasticity see e.g. Lewis (2019, 2021, forthcoming); Brunnermeier et al. (2021); Miescu (2021). Most importantly, Lewis (2019) also identifies the effects of the Fed policies from high-frequency financial data, and, remarkably, finds similar four dimensions of monetary policy. This is notable, because his approach is very different from the present paper. Lewis exploits the intraday time variation of the asset price volatility on the days of FOMC

announcements. On each of these days he fits a separate time series model and performs a separate identification. By contrast, here each FOMC announcement contributes only one observation and I rely on contrasting financial market reactions across the announcements.

Economists commonly assume Gaussian shocks, where shock independence boils down to their orthogonality. Consequently, in the Gaussian case the researcher needs additional identifying assumptions to choose among the infinity of orthogonal rotations of the shocks. By contrast, in models with statistical identification, such as the non-Gaussian or heteroskedastic cases, the rotations are no longer equivalent and one can discriminate among them based on the data, for example using the likelihood function. This does not preclude imposing identifying restrictions or informative Bayesian priors. I do not do it in this paper but it would be a straightforward extension.

The fact that in the non-Gaussian or heteroskedastic case the likelihood function discriminates among the shock rotations sidesteps some controversial issues, such as the critique of the sign restrictions by Baumeister and Hamilton (2015), or the challenges of doing inference in set-identified models (e.g Giacomini and Kitagawa, 2021). However, since these statistical methods pin down the shocks only up to sign and permutation, in Monte Carlo methods one needs to address the technical challenges of shock normalization (Waggoner and Zha, 2003) and label switching, and this paper shows how to do it.

Section 2 presents the data, highlighting their excess kurtosis. Section 3 lays out the baseline econometric model and explains the identification with a simple example. Section 4 reports the estimation results for the baseline model. Section 5 relaxes the key assumption of independence in the baseline model. Section 6 estimates models with larger information sets and different numbers of structural shocks. Section 7 tracks the longer term effects of the shocks using daily local projections. Section 8 concludes.

2 Data

The data on high-frequency financial market reactions to FOMC announcements come from the widely-used dataset of Gürkaynak et al. (2005) (GSS from now on) updated by Gürkaynak et al. (forthcoming). This dataset contains the changes of financial variables in a 30-minute

window around FOMC announcements (from 10 minutes before to 20 minutes after the announcement). The sample studied here contains 241 FOMC announcements from 5 July 1991 to 19 June 2019.

In the baseline analysis I consider a vector of four variables (later I also extract factors from a larger set of variables). I refer to the variables using their well-known GSS database identifiers. MP1, or the first fed funds future adjusted for the number of the remaining days of the month (see GSS for details) is the expected fed funds rate after the meeting. ONRUN2 and ONRUN10 are the 2- and 10-year Treasury yields. Finally, SP500 is the Standard and Poors 500 blue chip stock index.

The choice of MP1, ONRUN2 and ONRUN10 follows Swanson (2021), who finds that these three variables approximately span the target, path and LSAP factors that he constructs. I add the SP500 in order to capture the effects beyond the yield curve.

Figure 1: The empirical distributions of the baseline variables.

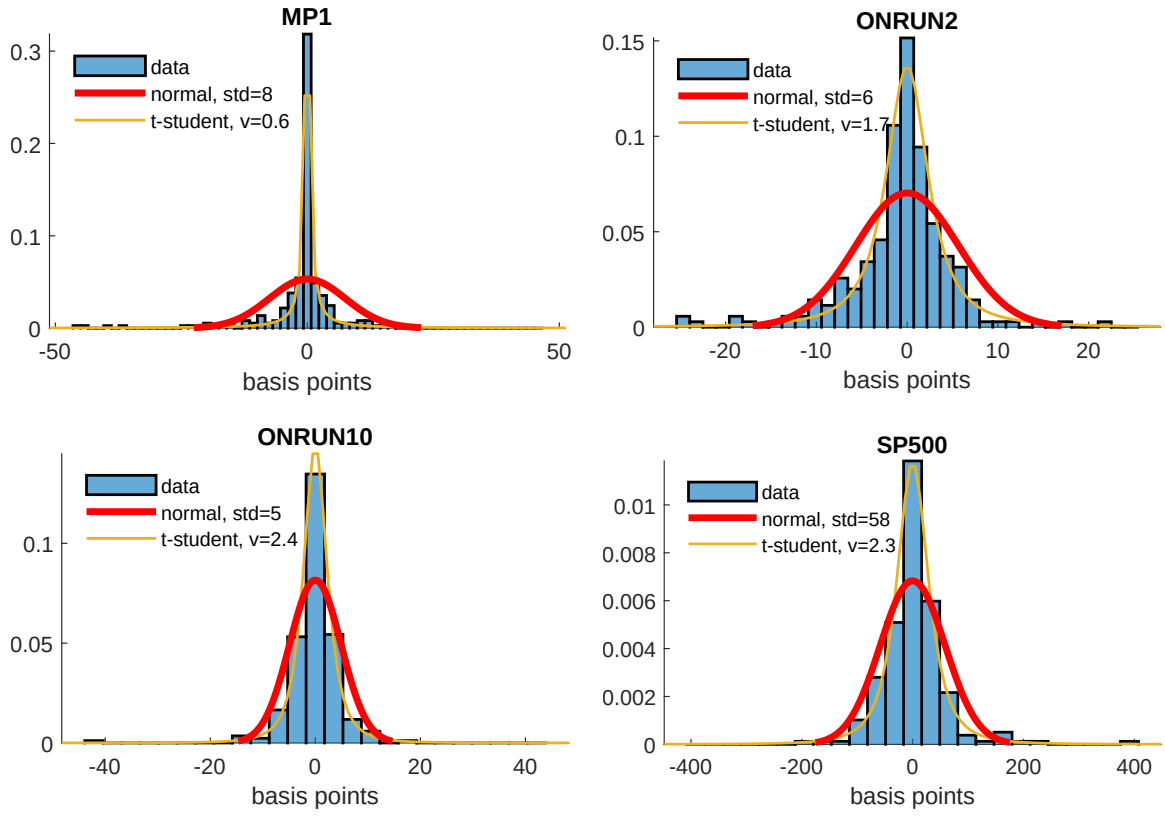

Note. Each plot contains the histogram of the data, the Gaussian density and the Student-t density each fitted into the data by maximum likelihood. The histograms are scaled so that they integrate to 1.

The responses of the four baseline variables to FOMC announcements are very non-Gaussian. Figure 1 reports, for each variable, the histogram, a Gaussian density and a Student-t density each fitted into the data by maximum likelihood. We can clearly see that the Gaussian densities, plotted in red, fit the histograms poorly. First, the Gaussian distributions predict too few near-zero observations. Second, the observed 4-, 6- and even 8-standard deviation outliers are unlikely under the Gaussian distribution. The fitted Student-t densities, which agree with the histograms quite well, have very low shape parameters ($v = 0.6, 1.7, 2.3, 2.3$, respectively) implying very large departures from Gaussianity.

3 The baseline econometric model

The baseline model assumes that market responses to FOMC announcements are driven by independent t-distributed shocks:

$$y_t = C' \, u_t, \qquad\qquad u_{n,t} \sim \text{i.i.d.} \mathcal{T}(v). \tag{1}$$

$y_t = (y_{1,t}, ..., y_{N,t})'$ is a vector of N variables observed at time t. $u_t = (u_{1,t}, ..., u_{N,t})'$ is a vector of unobserved, structural (i.e. uncorrelated) shocks. C is an $N \times N$ matrix whose i, j-th element $C(i, j)$ contains the effect of shock i on variable j. Equation (1) is a special case of a Structural VAR with no lags of y_t.[1] $\mathcal{T}(v)$ denotes the Student-t density with v degrees of freedom and the probability density function

$$p(u_{n,t}) = c(v) \left(1 + u_{n,t}^2 / v\right)^{-\frac{v+1}{2}}, \tag{2}$$

where $c(v) = v^{-1/2} B\left(\frac{1}{2}, \frac{v}{2}\right)^{-1}$ is the integrating constant, with $B(\cdot, \cdot)$ denoting the beta function.

A sample of T observations satisfies

$$Y = U \, C, \tag{3}$$

[1] Lags of y_t do not help predict y_t. Bauer and Swanson (2022) argue that y_t can be partly predicted (in sample) by certain other lagged variables but that this is inconsequential for studying the high-frequency effects of FOMC announcements on financial variables.

where Y is the $T \times N$ matrix with y_t' in row t and U is the corresponding $T \times N$ matrix of structural shocks. It is convenient to reparameterize the model in terms of $W = C^{-1}$, so that we can write $YW = U$. The log-likelihood of the sample Y is

$$\log p(Y|W, v) = T \log |\det W| - \frac{v+1}{2} \sum_t \sum_n \log(1 + u_{n,t}^2/v) + TN \log c(v), \tag{4}$$

where $u_{n,t} = y_t' w^n$, with w^n the n-th column of W. By maximizing the likelihood (4) we can estimate the set of shocks U and their effects $C = W^{-1}$. U and C are identified up to reordering and flipping the signs. The identification of this model depends crucially on non-Gaussianity and a sufficient degree of independence of the shocks.

3.1 The intuition behind the identification

The purpose of this section is to provide a simple illustration how structural relationships get revealed in the data in the presence of excess kurtosis and a sufficient degree of independence. For formal proofs that non-Gaussianity (of a more general form) of all but one shocks implies identification see e.g. Lanne et al. (2017), Proposition 2, or the discussion in Sims (2021).

For a simple illustration, consider a market for good A. Market prices P and quantities Q are determined by demand and supply, each subject to shocks. ΔP and ΔQ are the innovations in P and Q in response to shocks. Can we identify the slopes of the demand and supply curves from the data on ΔP and ΔQ?

Consider two structural models. In Model 1 the demand schedule is flat and the supply schedule is steep, while in Model 2 it is the reverse. Models 1 and 2 satisfy equation (5) with coefficients C_1 and C_2 respectively,

$$\begin{pmatrix} \Delta Q \\ \Delta P \end{pmatrix} = C'_{i\in\{1,2\}} \begin{pmatrix} s \\ d \end{pmatrix}, \text{ with } C_1' = \begin{pmatrix} 0.94 & 0.33 \\ -0.14 & 0.99 \end{pmatrix}, \quad C_2' = \begin{pmatrix} 0.14 & 0.99 \\ -0.94 & 0.33 \end{pmatrix}, \tag{5}$$

where s is a supply shock and d a demand shock. In Model 1 a unit supply shock s increases the quantity supplied by 0.94 while the market price falls by 0.14, revealing a flat demand curve with the slope of $-0.14/0.94 \approx -0.15$. The slope of the supply curve is $0.99/0.33 = 3$.

In Model 2 the slopes are -6.7 and 0.33 respectively. Panels A and B of Figure 2 plot these demand and supply curves.

Figure 2: Stylized example: demand and supply of good A.

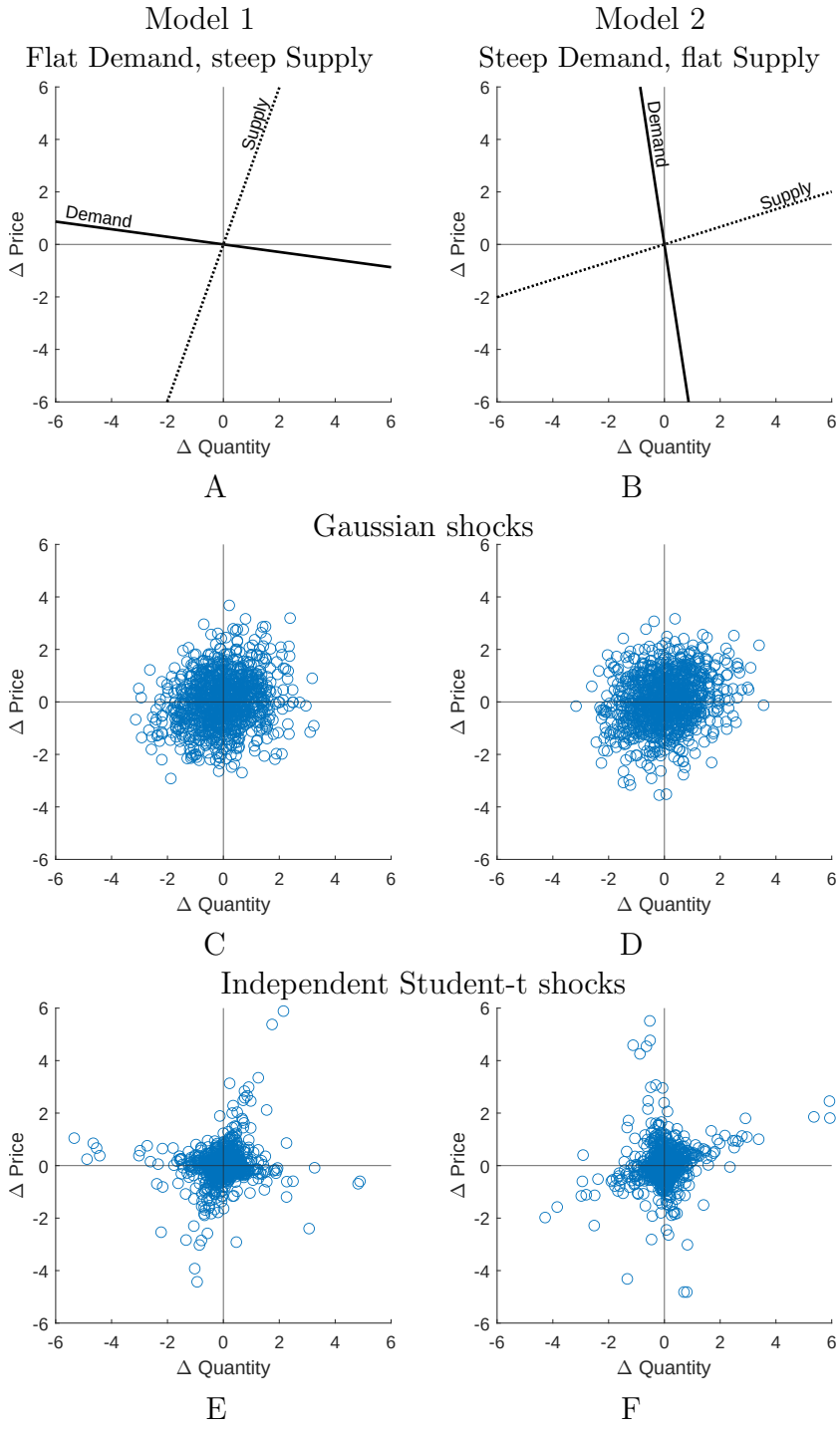

Figure 2: Continued

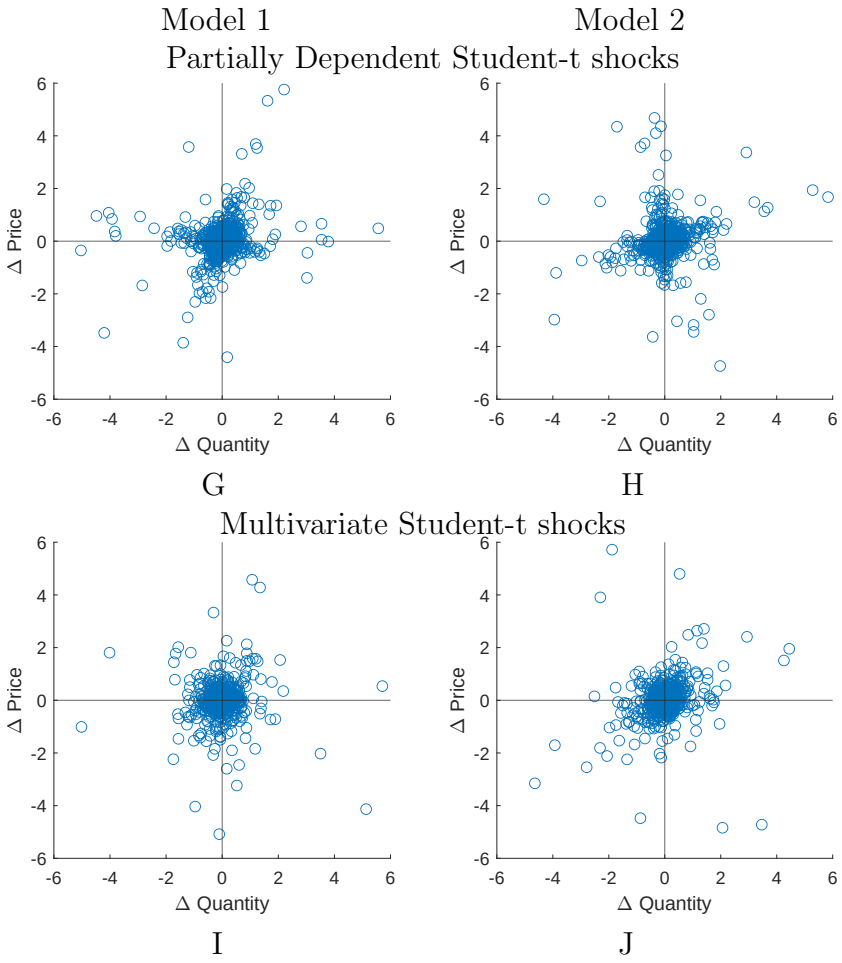

Note. Each scatter plot has 1000 observations. The samples in the left column are generated from (5) with coefficients C_1, and the samples in the right column are generated with coefficients C_2. In panels C and D the shocks d and s are independent Gaussian with mean 0 and variance 1. In panels E and F the shocks d and s are independent Student-t with mean 0, scale parameter 1 and shape parameter $v = 1.5$. In panels G and H the shocks d and s are drawn from the Partially Dependent Multivariate t distribution defined in section 5, with mean 0 and parameters $v_0 = 0.85$ and $\bar{v} = 0.65$. In panels I and J the shocks are drawn from the Multivariate Student-t with mean 0, scale parameter identity matrix and shape parameter $v = 1.5$. Before feeding to the model, the shocks are re-scaled so that their sample standard deviations equal 1. In all scatter plots, ΔP and ΔQ have sample mean zero, sample variance 1 and sample correlation 0.2.

When the shocks s and d are Gaussian, we cannot identify the slopes from the data on ΔP and ΔQ. The second row of Figure 2 presents the combinations of ΔP and ΔQ obtained from Model 1 in panel C and from Model 2 in panel D, when the shocks d and s are drawn from independent Gaussian distributions with mean 0 and variance 1. In this example $C_1 \times C_1' = C_2 \times C_2' = \left(\begin{smallmatrix} 1 & 0.2 \\ 0.2 & 1 \end{smallmatrix}\right)$. Consequently, in both cases $(\Delta P, \Delta Q)$ are Gaussian

with the same first two moments, (0, 0) and $\left(\begin{smallmatrix}1 & 0.2\\ 0.2 & 1\end{smallmatrix}\right)$, so the samples look the same.

However, when shocks s and d are independent Student-t, the situation changes. Now Models 1 and 2 produce systematically different combinations of ΔP and ΔQ. This is illustrated in the third row of Figure 2. The samples in the third row are generated from (5) but this time shocks d and s are drawn from independent Student-t distributions with mean 0 and shape parameter $v = 1.5$. For comparability with the previous example, the drawn shocks are re-scaled to ensure that their sample variance is 1. Hence, $(\Delta P, \Delta Q)$ continue to have the same first two sample moments, (0, 0) and $\left(\begin{smallmatrix}1 & 0.2\\ 0.2 & 1\end{smallmatrix}\right)$. Nevertheless, the samples in panels E and F look very differently from each other and even an observer lacking any statistical training will have no problem matching each sample with the correct structural model.

What helps here is the high kurtosis of the Student-t distribution, i.e. the fact that the shocks are often tiny, but sometimes large. For an outlying observation, chances are that only one of the shocks was large, while the other was tiny. Hence, these observations cluster around the demand and supply schedules, revealing their slopes.

Figure 3: Stylized example: information in the likelihood function of the data from panel E of Figure 2.

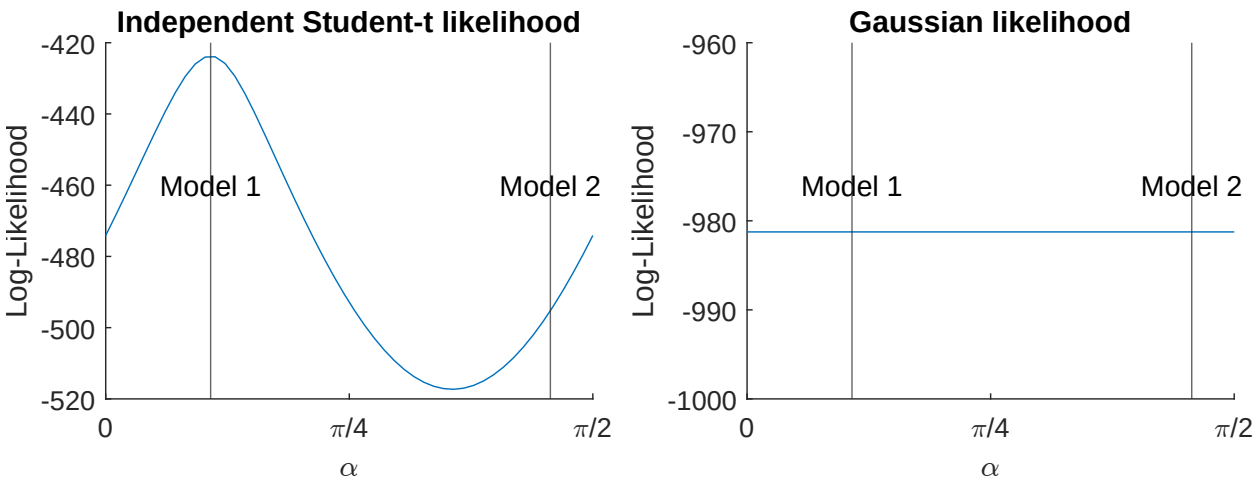

Note. Likelihood of the sample in panel E of Figure 2, as a function of the rotation angle α. $\alpha = 0$ corresponds to the Choleski decomposition of the sample variance of Y. Left panel: Independent Student-t likelihood given in (4). Right panel: Gaussian likelihood.

Obviously, if we can identify the structural model visually, we can also do it numerically

by evaluating the likelihood function. Let Y be the $T \times 2$ matrix collecting the data on prices and quantities from panel E of Figure 2, i.e. generated from Model 1. Let U be the $T \times 2$ matrix with orthogonal shocks. We can decompose Y into orthogonal shocks in infinitely many ways because

$$Y = UC = UQ(\alpha)Q(\alpha)'C = \tilde{U}\tilde{C} \qquad \text{for any} \qquad Q(\alpha) = \begin{pmatrix} \sin\alpha & \cos\alpha \\ -\cos\alpha & \sin\alpha \end{pmatrix} \tag{6}$$

where $U'U = I = \tilde{U}'\tilde{U}$. Parameter α indexes all models that fit the data Y while implying different slopes of demand and supply. All these models have the same likelihood if we incorrectly assume that the shocks are Gaussian. However, the Student-t likelihood discriminates between these alternative models. This is illustrated in Figure 3. The log-likelihood of the data from panel E implied by the Student-t distribution of shocks, given in (4), peaks at the rotation angle α that corresponds to Model 1. On the other hand, a researcher who wrongly assumes the Gaussian model would not be able to discriminate between the models, as the Gaussian likelihood is the same for any value of α. The Gaussian likelihood depends only on the first two moments and all values of α yield the same first two moments. However, incorrect values of α imply that demand and supply shocks must exhibit particular relations (such as a positive co-kurtosis), in order to match the data in panel E. This violates the independence of the shocks and hence gets penalized in the Independent Student-t likelihood.

The identification relies crucially on the shocks being independent. Figure 2 shows also what happens when the shock continue to have marginal Student-t distributions but the independence assumption is relaxed. In particular, they are still orthogonal, but when one of the shocks is large in absolute value, the probability that the other shock is large in absolute value increases. This blurs the picture compared with the case of independence. In panels G and H the shocks are moderately dependent and the models are still identifiable, but less clearly so, because there are more cases when both shocks are large, producing outliers that lay far away from either of the curves. Finally, in panels I and J the shocks are extremely dependent, (they come from a 2-dimensional Multivariate Student-t distribution).

In this case the identification breaks down. An outlying observation is very likely to reflect a combination of a large demand and large supply shock, and it is not likely to lay on one of the curves. The samples generated from Models 1 and 2 are not systematically different. The likelihood as a function of α is again flat.

The rest of the paper investigates whether the non-Gaussianity of the FOMC policy surprises reveals the slopes of structural relations conditional on different Fed shocks. In this real-life case no bi-variate scatter-plot of the variables from the GSS dataset looks as clear as panels E and F of Figure 2, so clearly one needs to consider more than two shocks and one needs to reconsider the assumption of independence. For ease of exposition, I start with the case of independence and then show that relaxing independence changes little in this particular empirical application.

3.2 Estimation

I estimate model (1) and conduct inference on the structural shocks and their impacts on the variables. I use the maximum likelihood estimation to obtain the point estimates $\hat{W}$ and $\hat{v}$, the structural shocks $\hat{U} = Y\hat{W}$, the impact matrix $\hat{C} = \hat{W}^{-1}$ and other quantities discussed later. To assess the estimation uncertainty I estimate the model with the Bayesian approach under flat priors (so effectively I simulate the exact shape of the likelihood), using the Metropolis-Hastings algorithm.

3.2.1 Maximum likelihood

I maximize the likelihood function (4). The Online Appendix provides the analytical expression for the gradient. One peculiarity of model (1) is that it is only identified up to a permutation of the shocks and up to scaling each shock by +/-1. The likelihood $p(Y|W)$ is invariant to permuting the columns of W ($N!$ possibilities) and flipping their signs (2^N possibilities), and consequently it has $N! \times 2^N$ equally high modes. The maximization routine converges to one of these modes, $\hat{W}$, which corresponds to a particular ordering and signs of the shocks. I compute the asymptotic variance of $(\operatorname{vec}\hat{W}', \hat{v})'$ as $\mathcal{V} = (-\mathcal{H})^{-1}$, where $\mathcal{H}$ is the Hessian of the log-likelihood at $\hat{W}, \hat{v}$.

3.2.2 Bayesian estimation with the Metropolis-Hastings algorithm

Next I use the Metropolis-Hastings algorithm to draw a sample of parameter values from the distribution proportional to the likelihood. This has two purposes. First, I want to explore the shape of the likelihood function in order to detect potential identification problems. Second, I want the inference about nonlinear functions of W, such as the C, to be as precise as possible. With a sample from the Metropolis-Hastings algorithm I can assess the uncertainty about all quantities of interest precisely without relying on asymptotic approximations.

Simulation. I start the simulation from the maximum likelihood estimate $\hat{W}, \hat{v}$. I generate proposal draws with a random walk model with the innovation variance equal to the asymptotic variance $\mathcal{V}$ scaled to ensure the acceptance rate of about 20%. The scale is 0.66 in the baseline model. I generate 10,000,000 draws and keep every 10,000-th. This simulation takes less than 5 minutes on a standard laptop. The convergence of the Markov Chain is confirmed with the Geweke (1992) diagnostics.

Normalization. The Metropolis-Hastings chain may visit the neighborhoods of different modes. As a consequence, given a draw of W one does not know to what ordering and signs of the shocks it corresponds. The draw needs to be normalized, i.e. mapped into the same ordering and signs of the shocks as in $\hat{W}$. One of the contributions of this paper is to propose a practical procedure for doing this. I proceed in two steps. First, I fix the signs of the shocks for each permutation. Second, I pick one of the (up to) $N!$ permutations, choosing the one that has *the highest probability under the Gaussian approximation of the likelihood function around* $\hat{W}$.

Let $\tilde{W}$ denote a draw of W, let $p = 1, ..., N!$ index the permutations of the N columns of $\tilde{W}$, let $\tilde{W}_p$ denote the matrix obtained by the p-th permutation of the columns of $\tilde{W}$, let $\mathcal{V}_W$ denote the asymptotic variance of $\operatorname{vec} W$ (i.e., $\mathcal{V}$ without the last row and column) and let $F(x|m, V)$ denote the multivariate Gaussian density with mean m and variance V evaluated at the point x.

Algorithm 1 *Given a draw* $\tilde{W}$*, for each permutation* $\tilde{W}_p$*,* $p = 1, ..., N!$*:*

1. *Scale the columns of* $\tilde{W}_p$ *by +/-1 using the Likelihood Preserving normalization of Waggoner and Zha (2003) (their Algorithm 1), obtaining a sign-normalized matrix* $\tilde{W}_p^{LP}$.

2. *Evaluate* $f(p) = F(\operatorname{vec} \tilde{W}_p^{LP} | \operatorname{vec} \hat{W}, \mathcal{V}_W)$.

Take the $\tilde{W}_{p*}^{LP}$ *where* $p* = \arg\max_p f(p)$ *as the normalized* $\tilde{W}$.

In practice, a finite Markov Chain may visit the neighborhoods of only a subset of modes. In this case, rather than considering all the $N!$ permutations, I only consider the permutations of those columns of W that have multiple modes before the normalization. This speeds normalization up.

In the baseline model (defined below) estimated on the full sample the different modes of the likelihood are well separated by regions of very low likelihood. As a result, a 10,000,000 long chain with the standard, 20% acceptance rate is unlikely to visit the neighborhood of another mode. However, for some of the alternative models studied later the chains do visit the neighborhoods of multiple modes and the normalization is indispensable (in these cases I apply the Geweke (1992) diagnostics to the normalized draws of W).

4 Estimation results for the baseline model

I define y_t=(MP1, ONRUN2, ONRUN10, SP500), estimate model (1) by maximum likelihood and then simulate the shape of the likelihood.

Figure 4 reports the distribution of the elements of C obtained with the simulation. Vertical lines represent the maximum likelihood estimates and the histograms represent the distribution of the draws from the Metropolis-Hastings algorithm. The distributions look approximately Gaussian and, ex post, yield very similar inferences as the asymptotic distribution of the maximum likelihood estimates. However, next subsections report some models where the likelihood functions have less regular shapes and the simulation-based inference matters.

Figure 5 reports the distribution of the degree of freedom parameter v. The maximum

Figure 4: The distribution of C

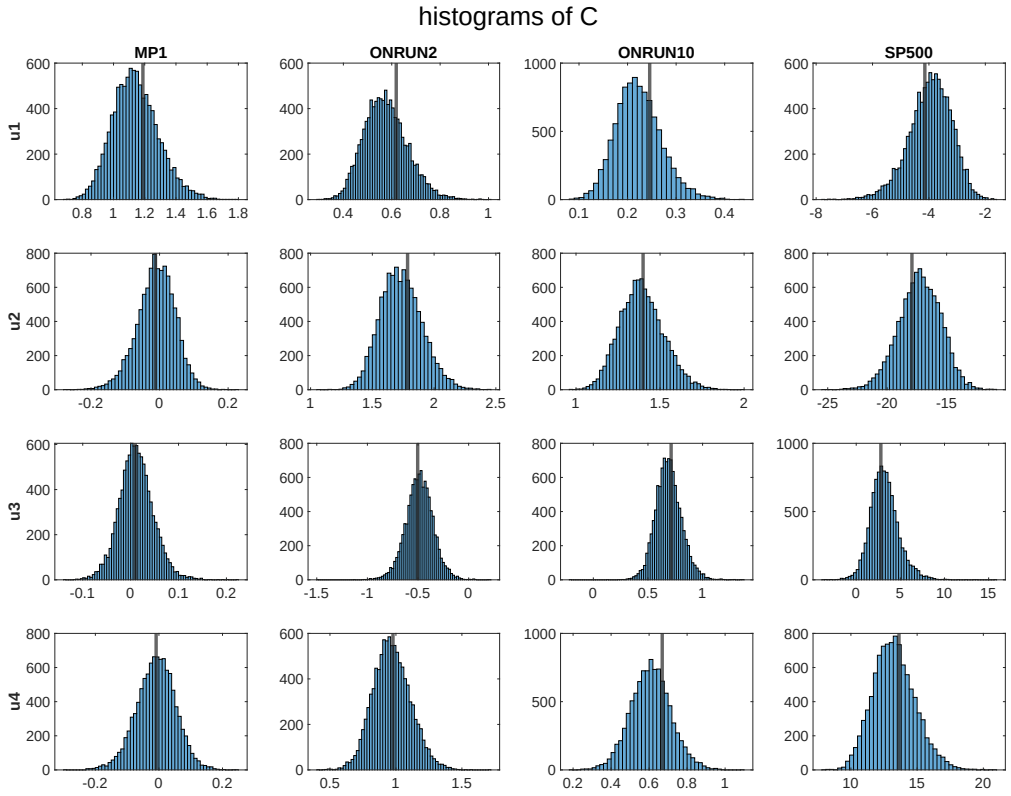

Note: Histograms of the elements of C based on the Metropolis-Hastings chain. Black vertical lines represent the maximum likelihood estimates.

Figure 5: The distribution of v

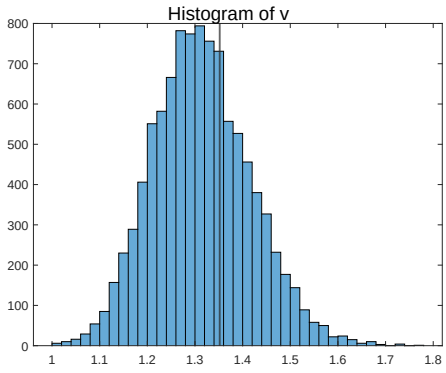

Note: Histogram of v based on the Metropolis-Hastings chain. The black vertical line represents the maximum likelihood estimate.

likelihood estimate is 1.35 and virtually all the probability mass lies between 1 and 2, implying a very leptokurtic distribution.

4.1 The impact effects of the four baseline shocks

Figure 6 reports C in a more convenient way. First, C gives the responses of Y to a unit shock, but it is easier to interpret and compare with the previous literature the effects of a one standard deviation shock. Although the standard deviation of u is not defined for the Student-t density with $v \leq 2$, one can always compute the sample standard deviation of $\hat{U}$ (obtained as $Y\hat{W}$). Therefore, in the following plots I re-scale the entries in each row of C by the sample standard deviation of the corresponding column of $\hat{U}$. Second, for simplicity I report only the modes and the 95% probability ranges (the ranges between quantiles 0.025 and 0.975). Third, I arrange the responses of interest rates into a yield curve, with the maturities on the x-axis. Figure 6 shows this more convenient presentation of C and Table 1 provides the underlying numbers for reference.

Figure 6: The responses of the variables to standardized shocks, 95% band.

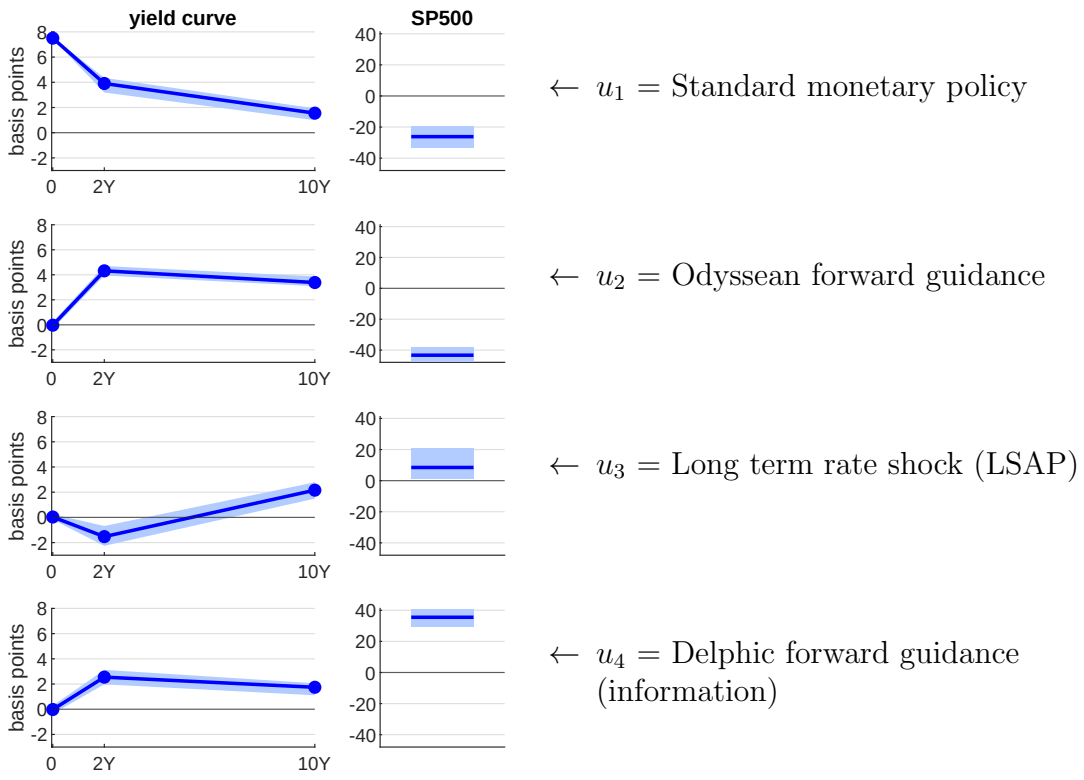

The shocks reported in Figure 6 are tightly estimated and have intuitive economic interpretations.

Table 1: The responses of the variables to standardized shocks

	MP1	ONRUN2	ONRUN10	SP500
u_1	7.50	3.91	1.55	-26.17
	(0.03)	(0.30)	(0.24)	(3.51)
u_2	-0.03	4.31	3.38	-43.31
	(0.14)	(0.19)	(0.20)	(2.47)
u_3	0.03	-1.53	2.16	8.47
	(0.11)	(0.39)	(0.33)	(4.88)
u_4	-0.02	2.55	1.74	35.51
	(0.16)	(0.30)	(0.24)	(2.82)

Notes. Standard deviations in parentheses. The same coefficients are reported graphically in Figure 6.

u_1 looks like a standard contractionary monetary policy shock. The fed funds rate increases by 7.5 basis points and other interest rates follow, with a weaker effect for longer maturities. The 2-year Treasury yield increases by almost 4 basis points and the 10-year Treasury yield by about 1.6 basis points. The SP500 index drops by 26 basis points.

u_2 looks like the effect of forward guidance. The fed funds rate does not change in the near term, but the 2-year yield increases by more than 4 basis points and the 10-year yield by 3.4 basis points in the half-hour window around the FOMC announcement. This shock is very contractionary and the SP500 drops by 43 basis points.

u_3 mostly affects the 10-year yield, while having has little effect on anything else, except the 2-year rate, which falls a little. However, I show later that in the second half of the sample this shock has a significant negative impact on the stock market and a positive impact on the 2-year rate. Furthermore, its large realizations coincide with important announcements of asset purchase policies, which justifies calling it an LSAP shock.[2]

Finally, u_4 moves the yield curve similarly as the forward guidance shock u_2, only is about two-thirds of the size. However, by contrast to u_2, this shock is accompanied by an *increase* in the SP500 index by 35 basis points, which can be rationalized by the presence of the Fed information effect. In particular, this shock perfectly matches the notion of the Delphic forward guidance of Campbell et al. (2012).

[2]Swanson (2021) also finds that his LSAP shock has an insignificant effect on the stock prices in the full sample.

Table 2: Variance decomposition

	MP1	ONRUN2	ONRUN10	SP500
u_1	**1.00**	**0.36**	**0.11**	**0.18**
	(0.00)	(0.04)	(0.03)	(0.04)
u_2	0.00	**0.44**	**0.53**	**0.48**
	(0.00)	(0.04)	(0.07)	(0.03)
u_3	0.00	0.05	**0.22**	0.02
	(0.00)	(0.03)	(0.06)	(0.03)
u_4	0.00	**0.15**	**0.14**	**0.32**
	(0.00)	(0.03)	(0.03)	(0.06)
Total	1.00	1.00	1.00	1.00

Note: Shares of the sample variance. Standard deviations in parentheses.

Since the shocks do not have a well-defined variance, also variance decompositions need to be taken with a grain of salt and we should expect them to be sensitive to outliers. Table 2 reports the variance decompositions of all variables, which should be interpreted with this caveat. u_1 is basically equivalent to MP1. In light of this, the federal funds rate surprises are a valid instrument for the standard monetary policy shock (e.g. Kuttner (2001); Bernanke and Kuttner (2005) use this instrument). However, the most important shock is the Odyssean forward guidance shock u_2, which accounts for 44% of the variation of 2-year bond yields and about a half of the variation of 10-year bond yields and stock prices in the half-hour windows around FOMC announcements. The third shock that is pervasive, in the sense that it accounts for non-trivial shares of multiple variables, is the Delphic forward guidance shock u_4. It accounts for about 15% of the variation of Treasury yields and one third of the variation of stock prices.

The effects of u_1 and u_2 on MP1 and Treasury yields reported in Table 1 are very similar to the effects of the target factor and path factor of GSS and Swanson (2021) (see e.g. Swanson's Table 3). This is in spite of the fact that I do not impose any of their identifying restrictions. Furthermore, the estimation uncertainty is very small. We can conclude that the maximum likelihood estimation that exploits the kurtosis of the data validates these earlier studies and their assumptions.

Another important lesson is that Fed information effects matter, as witnessed by the

nontrivial role of u_4, and they manifest themselves as the Delphic forward guidance. The theoretical models of Melosi (2017) and Nakamura and Steinsson (2018) focus on the information effects that accompany *current* fed fund rate changes, but my agnostic estimation picks up the information effects in the forward guidance.

4.2 The estimated shocks: the history

Figure 7: The estimated shocks over time.

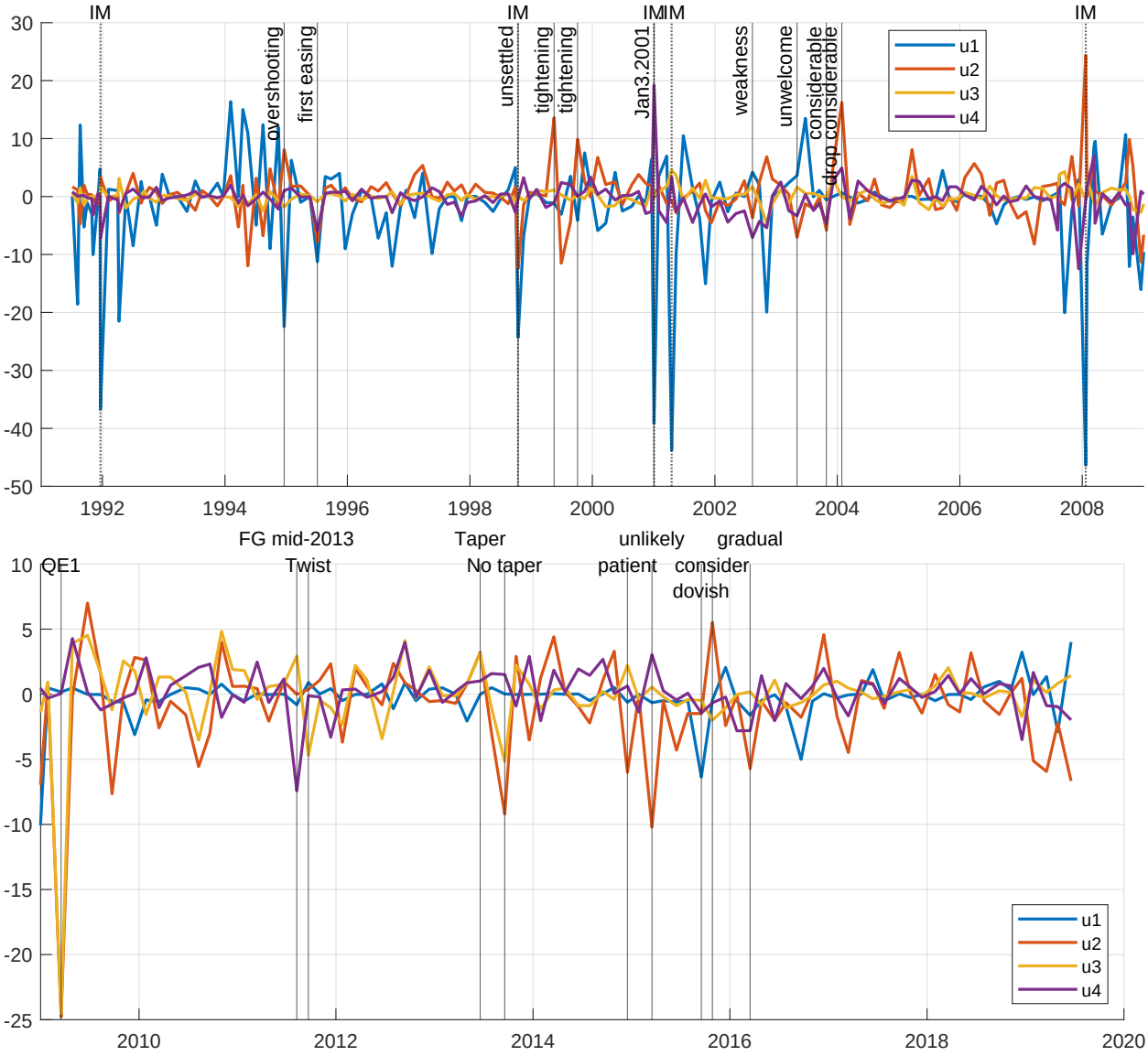

Note. IM: an "inter-meeting" announcement.

Figure 7 reports the history of the shocks over time. To facilitate interpretation, the

shocks are rescaled so that a one unit u_1 shock raises the MP1 by 1 basis point, a one unit u_2 and u_4 raises the ONRUN2 by 1 basis point, and a one unit u_3 shock raises the ONRUN10 by 1 basis point. The top panel of Figure 7 shows the pre-ZLB period 1991-2008 and the bottom panel the remaining period 2009-2019. Vertical bars highlight many of the same events as GSS and Swanson (2021). (For reference, the Online Appendix B provides the responses of the variables y_t to each of these events.)

The history of the standard monetary policy shock u_1 agrees with the accepted accounts. u_1 is essentially equal to MP1 and is also highly correlated with the GSS target factor/Swanson (2021) fed funds rate shock (rank correlation 0.76, linear correlation 0.95). Table 3 reports these and other correlations between various shocks. In the 1991-2008 plot we can see that, as is frequently noted, the largest realizations of standard policy shocks occur at inter-meeting announcements (labeled "IM" in the plot). Unsurprisingly, in the Zero Lower Bound period the standard monetary policy shocks are negligible.

The Student-t model interprets some of the forward guidance episodes as Odyssean, u_2 and some as Delphic, u_4, or the mix of both. Table 3 reports that the forward guidance shock of Swanson (2021) is highly positively correlated with both u_2 and u_4 (rank correlations of 0.74 and 0.48 respectively). The 1991-2008 plot in Figure 7 highlights the dates of the ten forward guidance episodes discussed in GSS (their Table 4, "Ten Largest Observations of the Path Factor"). They are labeled with the key word of the FOMC statement or a one-word description of its message. The Odyssean forward guidance, u_2 dominates the announcements marked 'overshooting' (December 1994, markets expect future tightening after Blinder's recent comments of 'overshooting'), 'unsettled' (October 1998), 'tightening' (May and October 1999) and 'drop considerable' (January 2004, dropping of the commitment to a 'considerable period' of the same policy). The Delphic forward guidance u_4 dominates the episodes labeled 'Jan3,2001' and 'weakness' (August 2002). The remaining highlighted announcements ('first easing', 'unwelcome' and 'considerable') are mixtures of both types of forward guidance.

The announcement on January 3, 2001 triggers the largest Delphic shock in the sample. This is a large inter-meeting rate cut that, as discussed in GSS, caused financial markets to mark down the probability or a recession and as a result expect higher rates down the road.

The GSS methodology picks it up as a combination of a target factor easing and a path factor (forward guidance) tightening. In this paper's methodology the forward guidance is of the Delphic kind and therefore reinforces the stock market gains rather than dampening them, which helps match the extremely large, 400bp increase in the S&P500. Since this u_4 shock is so large, I test the robustness of the results to dropping the January 3, 2001 observation from the sample and re-estimating the model. The results without this observation are basically unchanged. The correlation of the two estimates of u_4 on the remaining dates is more than 0.99 (Table 3).

In the announcement labeled 'weakness' on August 13, 2002 the FOMC stated that the balance of risks has shifted towards economic weakness. This stimulated both pessimism, reflected in stock market losses, and expectations of lower rates in the future. Therefore, while the announcement did not promise a rate cut explicitly, it worked as a Delphic forward guidance.

In the 2009-2019 plot in Figure 7 the largest Delphic shock is the 'mid-2013' announcement, issued on August 9, 2011, in which the FOMC stated that the "economic conditions ... are likely to warrant exceptionally low levels for the federal funds rate at least through mid-2013". It is intuitive that such a wording of the forward guidance is prone to trigger a Delphic interpretation (e.g. Del Negro et al. 2012 discuss the Delphic nature of this announcement). By contrast, the forward guidance episodes from December 2014 to March 2016 are either Odyssean, u_2 or mixes of Delphic and Odyssean.

Interestingly, the 'dovish' announcement on September 17, 2015, which is a major forward guidance shock in Swanson (2021), does not show up as such here. On that day markets priced in some probability that the Fed would raise the rates for the first time since 2008. The Fed did not change the rates and the MP1 dropped by 6.4 basis points upon the announcement. This is interpreted here as a standard fed funds rate shock u_1 of -6.4 basis points, accompanied by a mix of small Odyssean and Delphic forward guidance shocks of -1.5 basis points each. However, there are few other so clear discrepancies between the two approaches.

The largest by far LSAP shock u_3 accompanies the announcement of the expansion of the QE1 program (March 18, 2009). I check the robustness of the results to omitting this

observation, but all the lessons remain almost unchanged (see the second line of Table 3). As in Swanson's analysis, this shock is accompanied by a large expansionary Odyssean forward guidance shock. Another sizable expansionary LSAP shock happens at the announcement of the 'Operation Twist' (September 21, 2011). Finally, there is first a contractionary and then an expansionary LSAP shock during the "taper tantrum" episode, the first on June 19, 2013 ('taper') the second on September 18, 2013 ('no taper'). Also consistently with Swanson's findings, there are no expansionary LSAP shocks during the announcements of QE2 and QE3 programs.

Table 3: Pairwise rank and linear correlations with baseline shocks u_1, u_2, u_3 and u_4

	Obs.	u_1	u_2	u_3	u_4
Changing the sample					
Drop January 3, 2001	240	u_1: 0.998 *(1.000)*	u_2: 0.998 *(0.999)*	u_3: 0.988 *(0.995)*	u_4: 0.997 *(0.999)*
Drop QE1 (March 18, 2009)	240	u_1: 0.99 *(1.00)*	u_2: 0.99 *(1.00)*	u_3: 0.95 *(0.95)*	u_4: 0.96 *(0.98)*
Sample 1999-2004	120	u_1: 0.93 *(0.98)*	u_2: 0.89 *(0.95)*	u_3: 0.91 *(0.94)*	u_4: 0.97 *(0.99)*
Sample 2005-2019	120	u_1: 0.94 *(1.00)*	u_2: 0.82 *(0.78)*	u_3: 0.88 *(0.97)*	u_4: 0.96 *(0.98)*
Other papers					
Swanson (2021)	241	ff: 0.76 *(0.95)*	fg: 0.75 *(0.80)*	lsap: -0.66 *(-0.84)*	fg: 0.47 *(0.49)*
JK (2020) FF4	221	MP: 0.48 *(0.69)*	MP: 0.62 *(0.44)*	MP: -0.05 *(-0.04)*	CBI: 0.58 *(0.65)*
JK (2020) 1stPC	237	MP: 0.50 *(0.64)*	MP: 0.69 *(0.56)*	MP: -0.06 *(0.02)*	CBI: 0.77 *(0.81)*

Note. Rank (Spearman's) correlations on top, regular font; linear (Pearson's) correlations below, in brackets, italics. 'ff', 'fg' and 'lsap' stand for fed funds, forward guidance and large scale asset purchase shocks. 'MP' and 'CBI' stand for monetary policy and central bank information shocks.

Table 3 shows the correlations between u_1, u_2, u_3, u_4 and the related shocks identified with very different techniques by Swanson (2021) and Jarociński and Karadi (2020). The standard policy shock u_1 is highly correlated with Swanson's Fed Funds rate shock, the two forward guidance shocks u_2 and u_4 are both highly correlated with Swanson's single forward

guidance shock (he does not distinguish between Delphic and Odyssean forward guidance) and the LSAP shock u_3 is highly correlated with Swanson's LSAP shock (he scales his shock with the opposite sign). Jarociński and Karadi (2020) have a single catch-all monetary policy shock which is highly correlated both with u_1 and with u_2 (but does not capture asset purchases u_3). The Delphic shock u_4 is highly correlated with the central bank information (CBI) shock of Jarociński and Karadi (2020), which also picks up the positive correlation between interest rate surprises and stock price surprises. For the baseline CBI shock, which uses the fourth fed funds future (FF4) as the summary of the interest rate surprises, the correlation is 0.58. For the CBI shock based on the first principal component of futures with maturities up to 1 year as the summary of interest rate surprises, (reported by Jarociński and Karadi, 2020 in the Appendix), the correlation is even higher, 0.77.

4.3 Results in subsamples

Estimation of the model on smaller sub-samples yields two corrections to the previous messages. First, in the earlier part of the sample there is some evidence of the standard information effects associated with the movements of the current fed funds rate (as in Melosi, 2017; Nakamura and Steinsson, 2018). These standard information effects do not replace or modify the Delphic forward guidance but appear as a separate shock substituting the LSAP shock. Second, the LSAP shock u_3 has a significant effect on the stock prices in the later part of the sample.

Figure 8 reports the responses of all variables estimated in the first half of the sample (left panel) and in the second half of the sample (right panel). The error bands in these smaller samples are wider. A number of differences between the left and the right panel show up. First, the standard policy shock is moves the yield curve in a similar way but is larger in the first sample (MP1 increases by 9 basis points) and smaller in the second sample (MP1 increases by less than 6 basis points). Second, in response to the Odyssean forward guidance shock u_2 medium and long rates move in parallel in the first sample, while the effect is hump-shaped in the second sample, with the 10-year rate moving much less. Third, the LSAP shock is non-existent in the first sample. Instead, the shock u_3 now resembles the standard information shock associated with the fed funds rate, but is not precisely estimated.

Figure 8: First vs second half of the sample

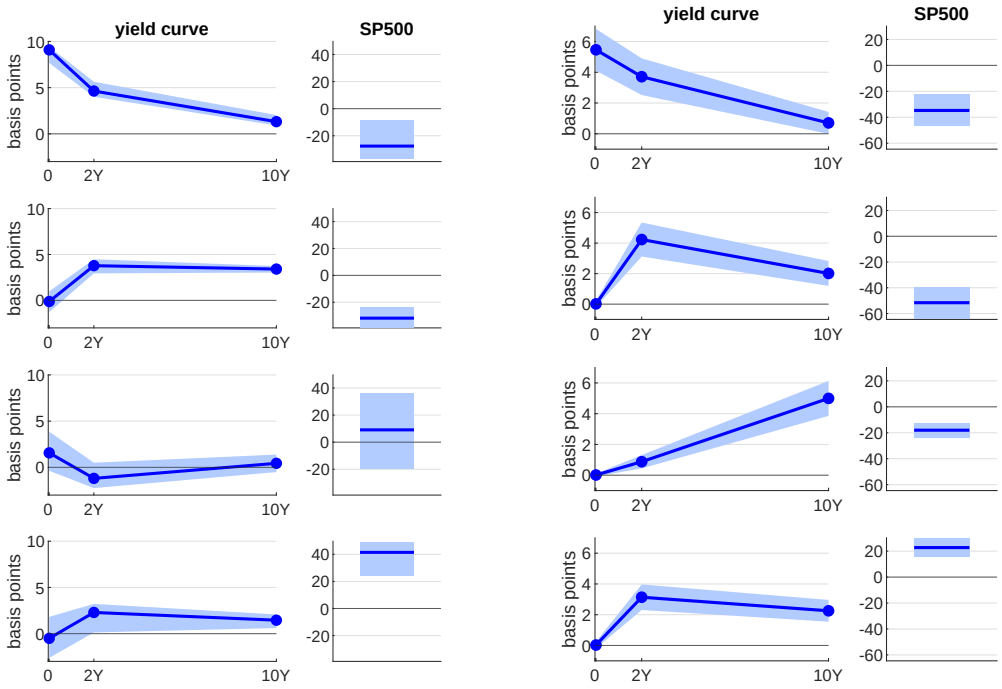

1991-2004 (120 obs.) 2005-2019 (121 obs.)

By contrast, the LSAP shock in the second sample is very pronounced and has a significant and intuitive effect on the stock prices. Finally, the Delphic forward guidance shock is broadly similar but it moves the stock prices more relatively to the interest rates in the first half of the sample.

Figure 9 reports the responses of all variables estimated on rolling windows of 100 observations. Many of these models are imprecisely estimated, but the overall tendencies are clear and quite intuitive. First, the standard monetary policy shock u_1 becomes smaller as the windows include more observations from the ZLB period. Second, for the Odyssean forward guidance u_2 we can see the gradual emergence of the 'hump-shaped' yield curve response noted above. Third, the shock u_3 is unstable and switches from being a standard information shock in the early windows (where it is a fed funds rate hike associated with a positive stock price response) to being a contractionary LSAP shock in the later windows. The switch occurs at the point where the rolling window includes for the first time the QE1 announcement of March 18, 2009. However, the same switch occurs, only several months later, when the QE1 announcement is omitted from the sample. Finally, the Delphic for-

Figure 9: Rolling window estimates of C

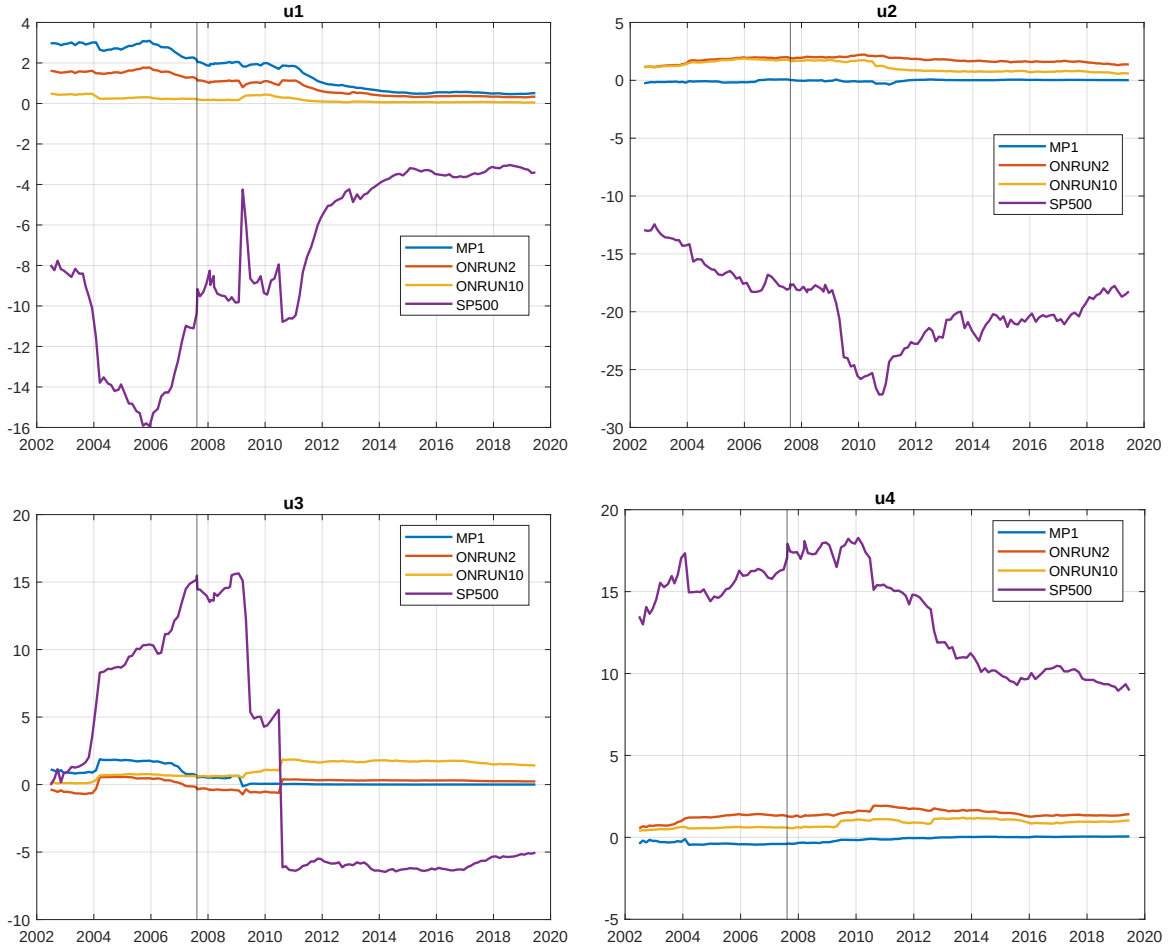

Notes. Each line plots the effect of shock u_i on variable j, $C(i,j)$ estimated on rolling samples of 100 observations. The horizontal axis shows the last observation of the rolling sample. The vertical line shows the beginning of the last sample.

ward guidance shock maintains similar features, while becoming slightly smaller in the later windows.

4.4 Are the estimated shocks leptokurtic and independent?

The marginal distributions of the estimated shocks $\hat{U}$ are very leptokurtic, consistently with the assumed model. Figure 10 shows the histograms of the estimated shocks $\hat{U}$ (blue bars) along with the plots of Student-t densities $\mathcal{T}(1.35)$, with the degrees of freedom parameter $v = 1.35$ that maximizes the likelihood function (red lines). We can see that the Student-t densities match the histograms quite well. But how independent are the estimated shocks?

Figure 10: The distribution of $\hat{u}$

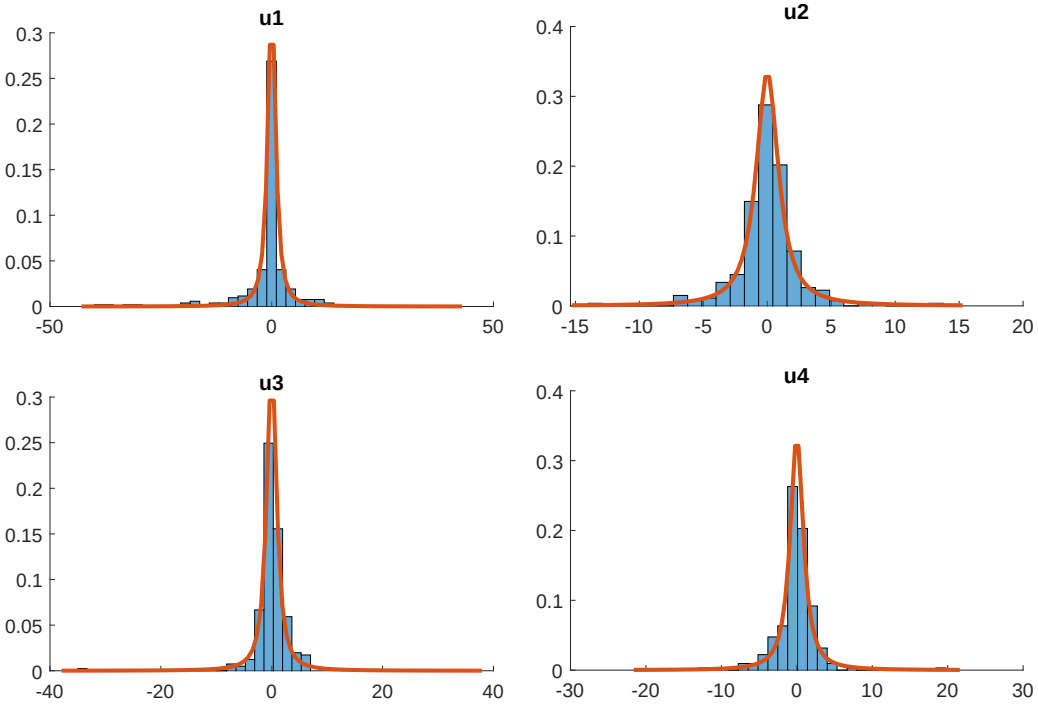

Table 4: Rank correlations and linear correlations between the shocks

Rank correlations					Linear correlations				
	u_1	u_2	u_3	u_4		u_1	u_2	u_3	u_4
u_1	1	-0.01	-0.01	0.02	u_1	1	-0.17	-0.07	-0.12
u_2	(0.92)	1	0.02	0.04	u_2	(0.01)	1	0.31	0.04
u_3	(0.90)	(0.77)	1	0.01	u_3	(0.25)	(0.00)	1	0.02
u_4	(0.70)	(0.52)	(0.83)	1	u_4	(0.06)	(0.49)	(0.76)	1

Note: Correlation coefficients above the diagonal, p-values in parentheses below the diagonal. Rank correlations (Spearman's correlations) in the left panel, linear correlations (Pearsons's correlations) in the right panel. The linear correlation between u_2 and u_3 drops from 0.31 to 0.06 if one omits the QE1 announcement.

Table 4 reports the correlations between the shocks and, at the same time, illustrates the perils of applying linear statistics to non-Gaussian variables. The rank (Spearman's) correlations, reported in the left panel are all negligible. However, the linear (Pearson's) correlations, reported in the right panel, are sometimes large. Especially striking is the correlation of 0.31 between u_2 (forward guidance shocks) and u_3 (LSAP shocks). Such a high correlation between Gaussian shocks would mean that they are systematically related and hence considering their effects in isolation makes little sense. However, for non-Gaussian

variables such a high linear correlations can happen by chance. In fact, in this case the linear correlation is almost entirely driven by a single observation, namely the announcement of the QE1 program in March 2009. After omitting this data point the linear correlation drops to 0.06, revealing that the shocks u_2 and u_3 are not in fact systematically linearly related.

Table 5: Rank correlations between the *squared* shocks

	$(u_1)^2$	$(u_2)^2$	$(u_3)^2$	$(u_4)^2$
$(u_1)^2$	1	0.16	0.12	0.19
$(u_2)^2$	(0.01)	1	0.19	0.15
$(u_3)^2$	(0.07)	(0.00)	1	0.23
$(u_4)^2$	(0.00)	(0.02)	(0.00)	1

Note: Correlation coefficients above the diagonal, p-values in parentheses below the diagonal.

Table 5 reports the rank correlations between the *squared* shocks, in order to understand if the shocks' absolute sizes are also independent, as assumed in model (1). It turns out that the shock sizes are not independent: in general large shocks are somewhat more likely to occur together. The rank correlations are positive and, with one exception, statistically significant at the 5% level. Given that independence plays a crucial role in the identification, it is important to revisit model (1) and check the robustness to relaxing the assumption of full independence (Montiel Olea et al., 2022).

5 Relaxing the assumption of independence

In this section I formulate and estimate an alternative model,

$$y_t = C' u_t, \qquad u_t \sim \mathcal{PDMT}(v_0, \bar{v}), \tag{7}$$

where $\mathcal{PDMT}(v_0, \bar{v})$ denotes the new Partially Dependent Multivariate t-distribution defined below. The PDMT distribution nests the Independent t and Multivariate t as extreme cases and spans all intermediate degrees of tail dependence between these extremes.

5.1 The PDMT distribution

I construct the PDMT through the following steps, inspired by Jones (2002); Shaw and Lee (2008); Jiang and Ding (2016). The construction is based on the fact that a t-distributed variate can be obtained by scaling a Normal variate by an inverse square root of a Chi-squared variate divided by its degrees of freedom:

$$\text{If } z \sim \mathcal{N}(0,1), \quad q \sim \chi^2(v) \quad \text{and } t = z\sqrt{\frac{v}{q}}, \quad \text{then } t \sim \mathcal{T}(v). \tag{8}$$

Consequently, a vector of independent t's can be constructed as

$$\left(z_1\sqrt{\frac{v}{q_1}},\ z_2\sqrt{\frac{v}{q_2}},\ \dots \right) \tag{9}$$

where $z_1, z_2, ...$ are independent standard Normal variates and $q_1, q_2, ...$ are independent Chi-squared variates with v degrees of freedom. The Multivariate t-distribution imposes a tight dependence on the tail behavior of all elements of the vector. A vector from the Multivariate t distribution can be constructed as

$$\left(z_1\sqrt{\frac{v}{q}},\ z_2\sqrt{\frac{v}{q}},\ \dots \right) \tag{10}$$

i.e. all the independent Normal variates are scaled by the same Chi-squared variate q. The new PDMT distribution is constructed as

$$\left(z_1\sqrt{\frac{v_0+v_1}{q_0+q_1}},\ z_2\sqrt{\frac{v_0+v_2}{q_0+q_2}},\ \dots \right) \tag{11}$$

where $q_0, q_1, q_2, ...$ are Chi-squared with $v_0, v_1, v_2, ...$ degrees of freedom. In the baseline case I will impose that $v_1 = v_2 = \cdots = \bar{v}$.

The $\mathcal{PDMT}(v_0, \bar{v})$ has the following attractive properties:

1. Each of its univariate marginal densities is $\mathcal{T}(v_0 + \bar{v})$. This is because the sum of a Chi-squared(v_0) and Chi-squared($\bar{v}$) is Chi-squared($v_0 + \bar{v}$).

2. When $v_0 = 0$ it collapses to a vector of Independent t-distributions with $\bar{v}$ degrees of

freedom.

3. When $\bar{v} = 0$ it collapses to a Multivariate t-distribution with v_0 degrees of freedom.

The disadvantage of the PDMT is that it does not have a tractable density.[3] Consequently, it needs to be studied using simulation methods.

5.2 Estimation

I estimate model (7) using Bayesian methods with diffuse priors and data augmentation.[4] I first rewrite it as

$$y_t = W^{-1\prime} Q_t^{-1/2} z_t, \quad z_t \sim \mathcal{N}(0, I_N) \tag{12}$$

where

$$Q_t = \text{diag}\left(\frac{q_{t0} + q_{t1}}{v_0 + \bar{v}}, \frac{q_{t0} + q_{t2}}{v_0 + \bar{v}}, \dots\right). \tag{13}$$

I treat the q_{tn} as missing data, and specify a "prior" or a likelihood for them that is $\chi^2(v_n)$, i.e. gamma $G(v_n/2, 2)$, given by

$$p(q_{tn}) = \Gamma(v_n/2)^{-1} 2^{-v_n/2} q_{tn}^{v_n/2-1} \exp(-q_{tn}/2) \tag{14}$$

where $n = 0, 1, ..., N$ and, in the baseline case, $v_1 = ... = v_N = \bar{v}$. Hence, the complete data likelihood in period t is

$$\begin{aligned} p(y_t, q_{1t}, ...q_{Nt}|W, v_0, ..., v_N) = |W^{-1\prime} Q_t^{-1} W^{-1}|^{-1/2} \exp\left(-\frac{1}{2} y_t' (W^{-1\prime} Q_t^{-1} W^{-1})^{-1} y_t\right) \\ \times \prod_{n=0}^{N} \Gamma(v_n/2)^{-1} 2^{-v_n/2} q_{tn}^{v_n/2-1} \exp(-q_{tn}/2) \end{aligned} \tag{15}$$

I specify priors for parameters $W, v_0, v_1, ...$ The prior for W is flat, $p(W) \propto 1$. The prior for v_n is $\mathcal{G}(\alpha_n, \beta_n) = \Gamma(\alpha_n)^{-1} \beta_n^{-\alpha_n} v_n^{\alpha_n - 1} \exp(-v_n/\beta_n)$. I use the noninformative priors $\alpha_n = 0$ and $\beta_n = \infty$ in the estimations reported below (I verified that using proper but weakly informative priors makes little difference to the results).

[3] Jones (2002) discusses a related distribution that does have a tractable density but notes that this seems to be an exception in this class of distributions.

[4] For a frequentist perspective on data augmentation see e.g. Jacquier et al. (2007).

I conduct inference on the parameters $W, v_0, v_1, ...$ using a version of the Metropolis-Hastings algorithm. At each step of the simulation I draw new W, v_n, q_{tn} for $n = 0, ..., N$ and $t = 1, ..., T$ from their respective conditional densities, conditioning on the most recent draw of the remaining quantities.

The conditional posterior of W is

$$p(W|Y, \cdot) \propto |W|^T \exp\left(-\frac{1}{2}\sum_t y_t' W Q_t W' y_t\right). \tag{16}$$

This posterior is nonstandard. To draw from it, I draw a candidate W^* from the Gaussian proposal density

$$f(W) = \mathcal{N}\left(\hat{w}, \kappa\mathcal{H}^{-1}\right) \tag{17}$$

where $\hat{w}$ is the mode of $p(W|Y, \cdot)$, $\mathcal{H}$ the Hessian of $\log p(W|Y, \cdot)$ and $\kappa \geq 1$ is a scalar. I derive the analytical expressions for the gradient and the Hessian of $\log p(W|Y, \cdot)$ using the methods of Magnus and Neudecker (2019).

The candidate draw is accepted with probability

$$\min\left(1, \frac{p(W^*|Y, \cdot)\, f(W)}{f(W^*)\, p(W|Y, \cdot)}\right) \tag{18}$$

and with the complementary probability I keep the previous draw W.

The conditional posteriors of q_{nt}, v_n are also non-standard densities, related to the Gamma density. Therefore, as the proposal density I use a Gamma density close to the target density. I draw from the proposal Gamma density and accept the draw with the appropriate acceptance probability as in (18). The Online Appendix provides the details.

The following results are based on a chain of 1,050,000 draws, of which I discard the first 50,000 and keep every 500th from the rest. I confirm the stationarity of the chain with the Geweke (1992) diagnostics. While the whole inference with the Independent t model (1) in the previous section takes seconds (maximum likelihood) or minutes (simulation), generating a 1,050,000-long chain for the PDMT takes a few hours.

5.3 Results

The PDMT model detects a nontrivial degree of tail dependence. Figure 11 reports the posterior distributions of the degree of freedom parameters. The common degrees of freedom v_0 are about 50% larger than the idiosyncratic degrees of freedom $\bar{v}$ (0.9 vs 0.6).

Figure 11: PDMT model: the posterior distributions of $v_0, \bar{v}$.

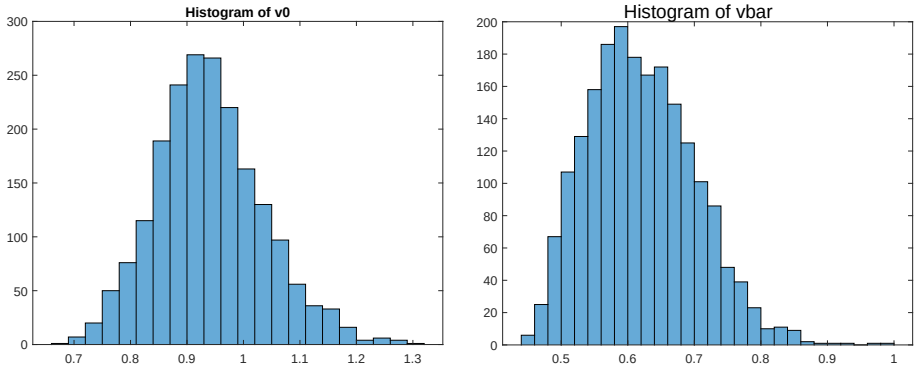

Common degrees of freedom Idiosyncratic degrees of freedom

The uncertainty about C increases in the PDMT model, but not dramatically. Figure 12 reports the 95% posterior bands for C in the PDMT model, together with the 95% bands and maximum likelihood estimates in the independent Student-t model (1) for comparison. We can see that the uncertainty bands are still quite tight and the bottom line is that the estimated shocks are the same.

To gauge the sensitivity to idiosyncratic degree of freedom $\bar{v}$ I push the model even further and re-estimate it imposing a restriction $\bar{v} = 0.3$ (i.e. cutting $\bar{v}$ by half) and $\bar{v} = 0.15$. As shown in Figure 13, these restrictions widen the uncertainty bands considerably, although the key features of the shocks are still distinguishable. Only when I try to push $\bar{v}$ even lower, the conditional posterior of W becomes too flat and the algorithm runs into numerical problems.

The key lesson from this section is that the shocks need not be fully independent to achieve meaningful identification. In this empirical application the baseline results are robust to relaxing the assumption of independence. Therefore, in the remainder of the paper I revert to the Independent t model for simplicity.

Figure 12: PDMT model: the responses of the variables to standardized shocks.

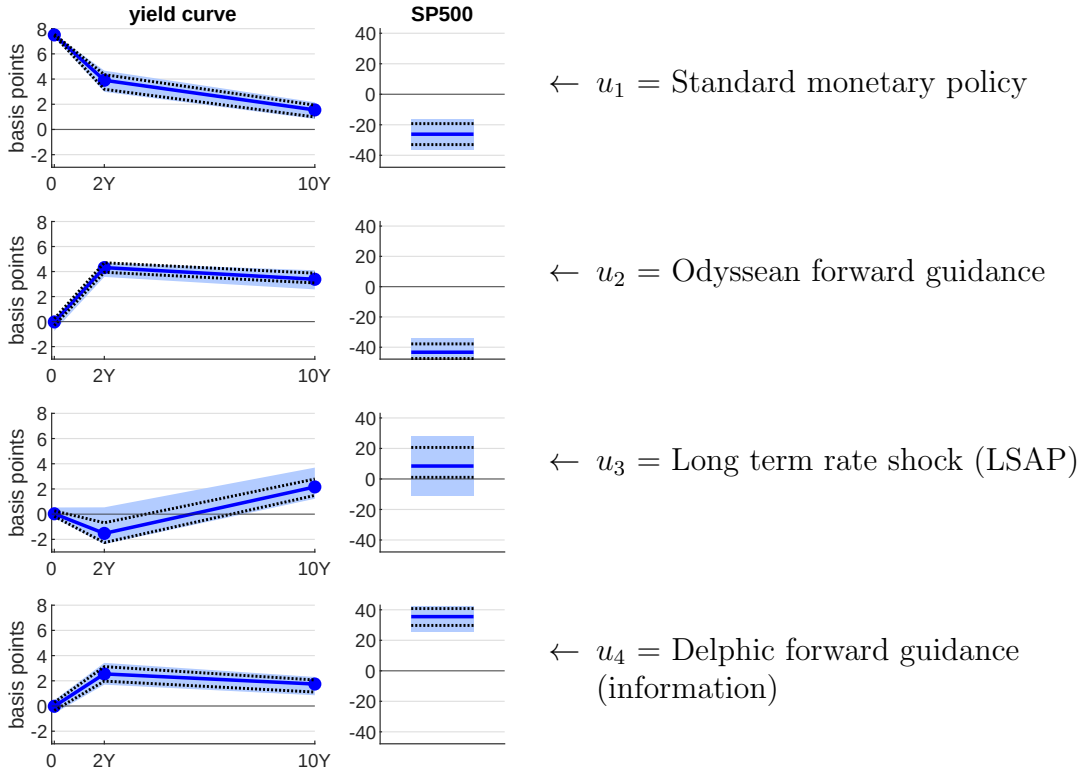

Notes: The blue areas show the 95% posterior probability bands in the PDMT model. The dotted lines show the 95% bands in the Independent t model. The blue solid lines show the maximum likelihood estimates in the Independent t model.

6 Using more information

6.1 Estimation with the principal components of interest rates

In this section I reestimate the baseline model replacing the three interest rates MP1, ONRUN2, ONRUN10 with the first three principal components extracted from a larger set of interest rates. I take eight variables from the GSS dataset: the first and third fed funds futures, the second through fourth eurodollar futures, 2-year, 5-year, and 10-year Treasury yields. In terms of the GSS identifiers, I specify

$$x = (\text{MP1, FF3, ED2, ED3, ED4, ONRUN2, ONRUN5, ONRUN10}). \tag{19}$$

This choice of variables follows Swanson (2021)'s choice of liquid instruments with maturities that do not overlap. I extract the first three principal components from x and plug them

Figure 13: PDMT model: restricting $\bar{v}$.

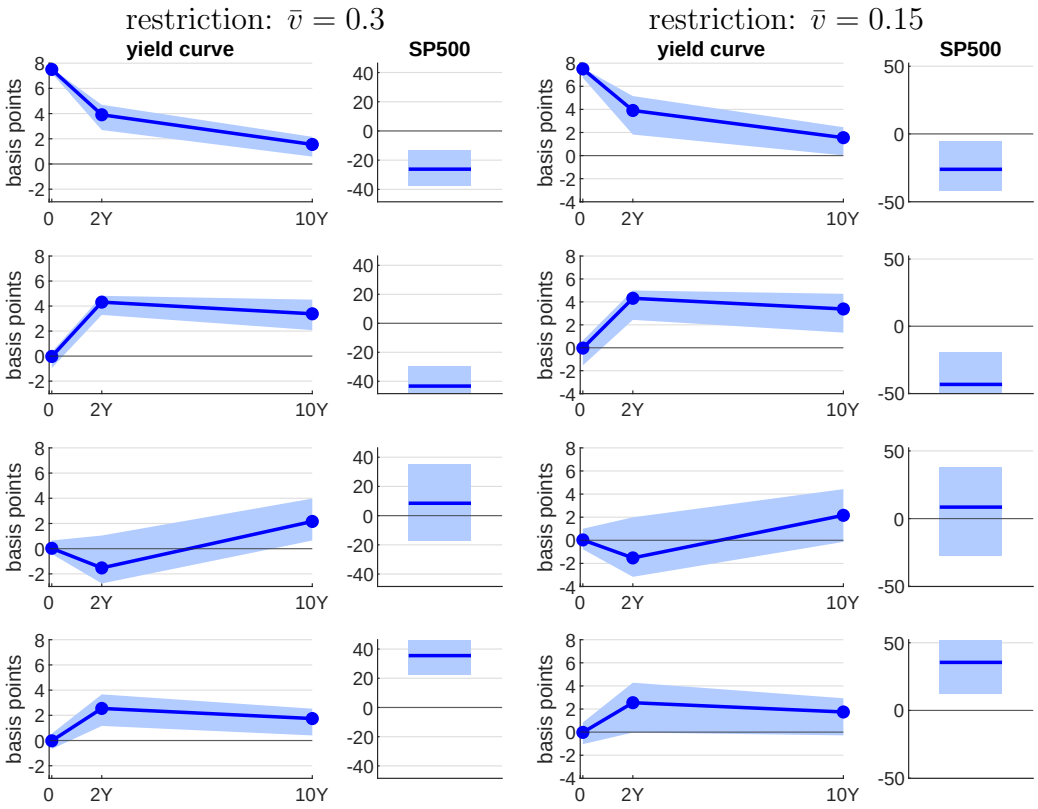

Notes: The blue areas show the 95% posterior probability bands in the PDMT model. The blue solid lines show the maximum likelihood estimates in the Independent t model.

into the model along with the SP500, i.e. I specify y=(PC1(x), PC2(x), PC3(x), SP500).

I estimate model (1) by maximum likelihood, obtaining four shocks and the matrix C containing their effects on the three principal components and on SP500. Then I multiply the coefficients of the principal components (i.e. the first three columns of C) by their loadings in the principal components analysis, thus backing out the effects of the shocks on the original GSS variables. Figure 14 reports the results.

We can see four shocks that are very similar as in the baseline case.[5] The model is now even more tightly estimated, which is intuitive if the principal components extraction removes some idiosyncratic noise. The new findings are about the intermediate maturities that were missing in the baseline specification. In particular, we can see that both Odyssean and Delphic forward guidance have the strongest effects on the fourth eurodollar future, i.e. on interest rate expectations approximately one year to the future.

[5]Table 7 reports their rank correlations with the baseline shocks, which range from 0.73 to 0.96.

Figure 14: The model with the principal components: responses of the variables to standardized shocks.

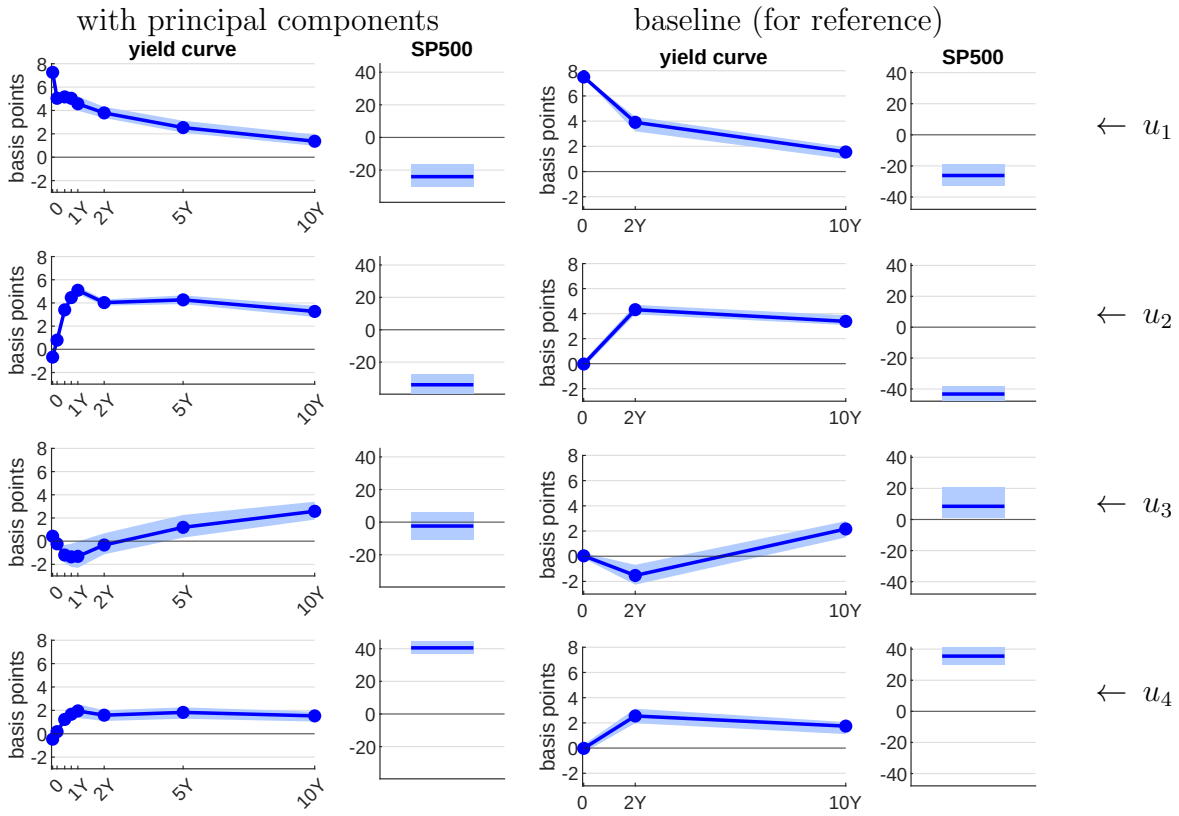

Notes: The blue areas show the 95% posterior probability bands and the solid lines with dots show the maximum likelihood estimates. The results are based on the Independent t model.

6.2 Models with three shocks

In this section I estimate models with three shocks. First, I drop the SP500 surprise and limit the analysis to the three principal components of interest rate surprises, y=(PC1(x), PC2(x), PC3(x)). This information set is the same as in Swanson (2021). It turns out that in this case I estimate basically the same shocks as Swanson (2021). Table 6 reports that the rank correlations between these shocks range from 0.83 to 0.95 and the linear correlations range from 0.94 to 0.97 (I normalize the lsap shock to be a tightening so for this shock the sign of the correlation is negative). Figure 15 shows the effects of the three shocks in the first column. We can see the intuitive effects of a standard policy shock, a forward guidance shock and an asset purchase shock. It is remarkable that one can recover Swanson's shocks by maximizing the Student-t likelihood only, without imposing his bespoke factor rotations.

This exercise serves as another statistical validation of Swanson's approach.

Figure 15: Models with three shocks: responses of the variables to standardized shocks.

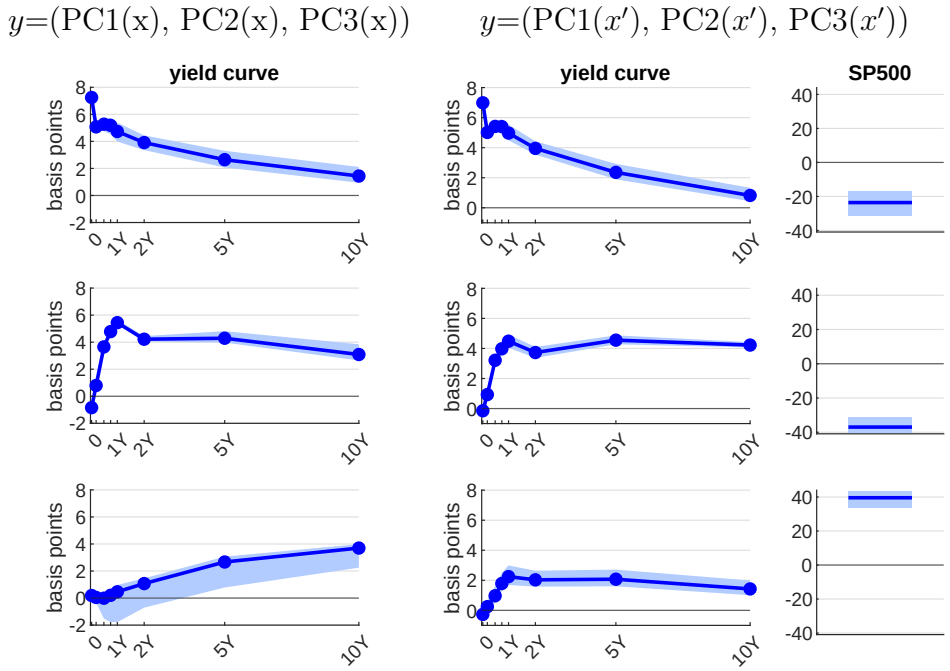

Notes: The blue areas show the 95% posterior probability bands and the solid lines with dots show the maximum likelihood estimates. The results are based on the Independent t model.

Table 6: Pairwise rank and linear correlations for models with three shocks

	Obs.	u_1	u_2	u_3
y=(PC1(x), PC2(x), PC3(x))				
Swanson (2021)	241	ff: 0.83 *(0.97)*	fg: 0.95 *(0.95)*	lsap: -0.88 *(-0.94)*
y=(PC1(x'), PC2(x'), PC3(x'))				
Baseline	241	u_1: 0.74 *(0.94)*	u_2: 0.97 *(0.98)*	u_4: 0.97 *(0.99)*

Note. Rank (Spearman's) correlations on top, regular font; linear (Pearson's) correlations below, in brackets, italics. 'ff', 'fg' and 'lsap' stand for fed funds, forward guidance and large scale asset purchase shocks.

In the second experiment, I include the stock price in the vector from which I extract three principal components. That is, I specify a nine-variable vector x', consisting of the

previous eight variables plus SP500,

$$x' = (\text{MP1, FF3, ED2, ED3, ED4, ONRUN2, ONRUN5, ONRUN10, SP500}). \tag{20}$$

I extract three principal components, specify y=(PC1(x'), PC2(x'), PC3(x')) and estimate model (1). This time the three shocks picked up by the maximum likelihood estimation are essentially the same as the standard policy (u_1), Odyssean forward guidance (u_2) and Delphic forward guidance (u_4) shocks in the baseline specification. This is clear both from the impact effects of the shocks, reported in the right panel of Figure 15 and from the high positive correlations with baseline u_1, u_2, u_4 reported in Table 6.

To sum up, a three shock model focused on the interest rates alone recovers the fed funds, forward guidance and LSAP shocks of Swanson (2021). A three shock model accounting for the stock prices as well recovers the fed funds, Odyssean forward guidance and Delphic forward guidance shocks.

6.3 Searching for more shocks

In this section I estimate models with five or more shocks. These exercises yield either additional Delphic shocks differing by the stock price responsiveness, or a new shock that mainly affects the exchange rate.

First, I extract five principal components from x' and specify y=(PC1(x'), PC2(x'), PC3(x') PC4(x'), PC5(x')). See the first panel of Figure 16. In this case the first three shocks remain unchanged, but instead of a single Delphic shock we now have two Delphic shocks, of which one moves the stock prices more relative to the yield curve, and another less.

Second, I specify a ten-variable vector x'', consisting of the previous nine variables plus the euro-dollar exchange rate,

$$x'' = (\text{MP1, FF3, ED2, ED3, ED4, ONRUN2, ONRUN5, ONRUN10, SP500, EURO}). \tag{21}$$

I extract five principal components from x'' and specify y=(PC1(x''), PC2(x''), PC3(x'')

Figure 16: Models with more shocks

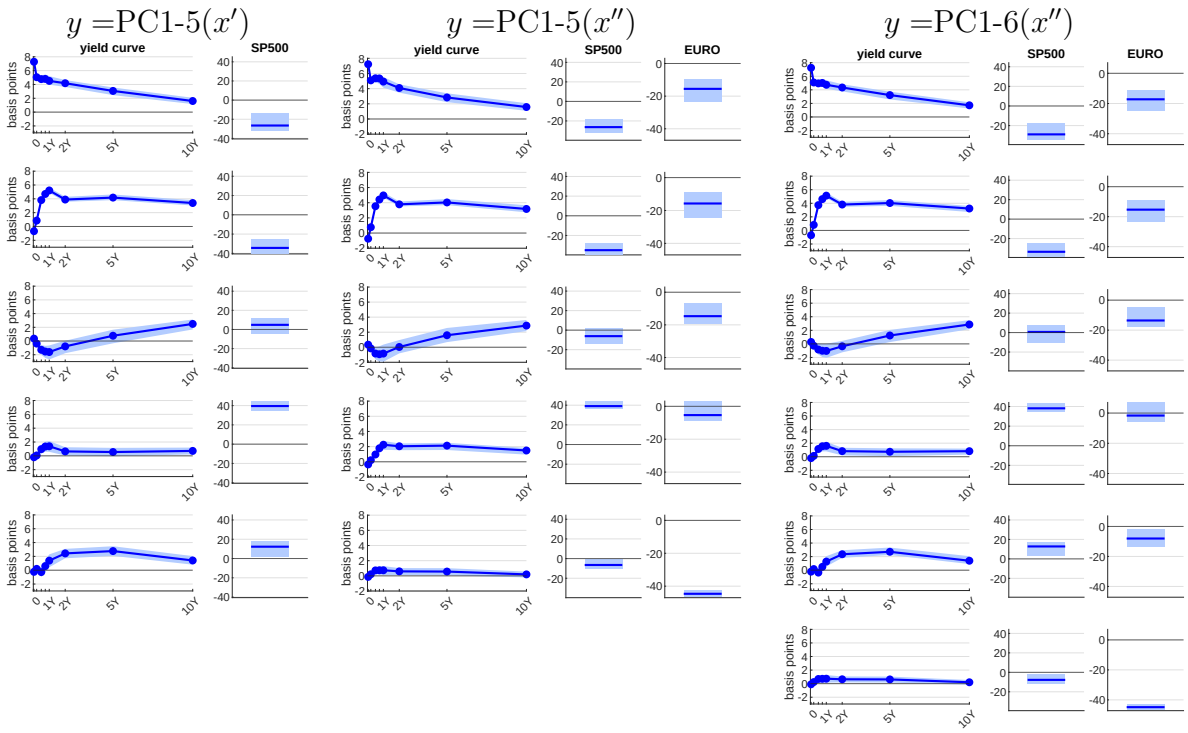

PC4(x''), PC5(x'')). See the second panel of Figure 16. In this case the first four shocks are again basically as in the baseline specification. Additionally, we can now observe the responses of the dollar. The first three shocks, standard policy, Odyssean forward guidance and LSAP shocks, have a similar effect on the dollar: it strengthens by about 15 basis points in each case. By contrast, the Delphic shock has an insignificant effect on the dollar. We also obtain a new, fifth shock which mainly affects the exchange rate, while having very small effect on the interest rates and stock prices.

In the third exercise I extract six principal components from x'' and include all of them in y. See the third panel of Figure 16. In this case we obtain the shocks familiar from the previous two exercises: two Delphic shocks and an exchange rate shock, in additional to the standard policy, Odyssean forward guidance and asset purchases.

Table 7 reports the rank correlations of the shocks obtained in the above exercises with the baseline shocks. In each case the first four shocks are highly correlated with the corresponding baseline shocks. The new Delphic shock is mainly correlated with the baseline Delphic shock (0.48). The new exchange rate shock is weakly negatively correlated with the LSAP shock

Table 7: Pairwise rank correlations with the baseline model shocks

	Obs.	u_1		u_2		u_3		u_4	
Model in Figure 14									
PC1-3(x),SP500	241	u_1:	0.90	u_2:	0.96	u_3:	0.73	u_4:	0.96
Models in Figure 16									
PC1-5(x')	241	u_1:	0.93	u_2:	0.89	u_3:	0.93	u_4:	0.77
		u_5:	0.03	u_5:	0.19	u_5:	-0.14	u_5:	0.48
PC1-5(x'')	241	u_1:	0.91	u_2:	0.92	u_3:	0.69	u_4:	0.97
		u_5:	0.00	u_5:	0.12	u_5:	-0.23	u_5:	-0.06
PC1-6(x'')	241	u_1:	0.93	u_2:	0.87	u_3:	0.92	u_4:	0.77
		u_5:	0.04	u_5:	0.18	u_5:	-0.12	u_5:	0.47
		u_6:	0.00	u_6:	0.14	u_6:	-0.23	u_6:	-0.07

Note. The first column identifies the models by the variable(s) included in y.

(-0.23) and very little with the other shocks.

7 Longer term effects: daily local projections

To study the effects of the four baseline shocks beyond the first thirty minutes after the FOMC announcement I estimate local projections:

$$x_{t+h} - x_{t-1} = \alpha + \beta_h^i u_{i,t} + e_t, \tag{22}$$

where x_t is a daily financial variable and t is day of the FOMC announcement. I consider horizons $h = 1, 3, 5, 10, 15, 20, 25$ business days. $u_{i,t}, i = 1, 2, 3, 4$ are the maximum likelihood estimates of the shocks implied by the baseline model above, rescaled so that a one unit u_1 shock raises the MP1 by 1 basis point, a one unit u_2 and u_4 raises the ONRUN2 by 1 basis point, and a one unit u_3 shock raises the ONRUN10 by 1 basis point. The shocks are included in the regressions one-by-one. β_h^i is the quantity of interest: the effect of a one unit shock. I estimate equation (22) with OLS and compute heteroskedasticity-robust errors. Figure 17 reports the results.

Three main lessons follow from these local projection results. First, the effects of the

Figure 17: The effects of the shocks on daily financial variables: local projections

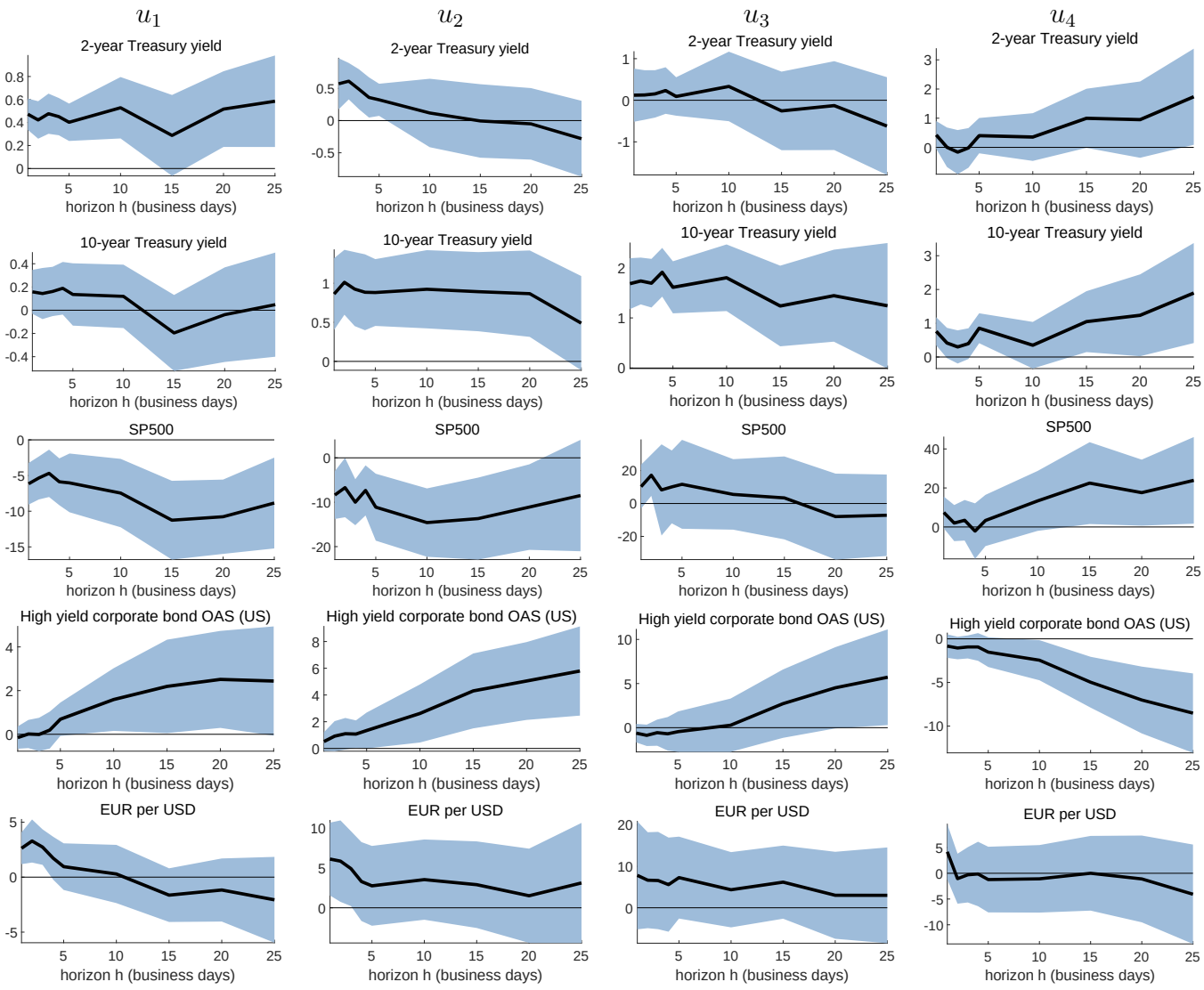

Note. The variables are in the same units as the shocks. 90% bands (+/-1.645 standard deviations)

shocks on interest rates and stock prices in the first 30 minutes given by the matrix C are not just temporary blips. They persist in the following days and weeks, and are statistically significant at many, though not all horizons. In particular, shocks u_1 and u_2 significantly increase the 2-year Treasury yield (with the elasticity of approximately 0.5) and depress the stock prices (with the elasticities of -6 and -8). Shocks u_2 and u_3 significantly increase the 10-year Treasury yields (with the elasticities of 1 and almost 2). The positive effect of the Delphic shock u_4 on Treasury yields and stock prices is marginally significant at some horizons and insignificant at others.

Second, the shocks gradually propagate through the financial system and with some delay get reflected in the corporate bond spreads. Especially the Odyssean and Delphic forward guidance shocks u_2, u_4 significantly affect the corporate bond spreads after a few weeks (in the opposite directions).

Third, the standard policy and forward guidance shocks u_1 and u_2 significantly strengthen the dollar vs the euro (with the elasticities of 3 and 6 respectively). The effect of the asset purchase shock u_3 is even larger according to the point estimates (the elasticity of 8), but estimated with a large uncertainty. The effect of the Delphic shock u_4 on the dollar is the weakest, it is actually zero at most horizons. This shock's weak impact on the exchange rate is consistent with the recently highlighted role of the dollar as a key barometer of financial market risk-taking capacity (Avdjiev et al., 2019). A positive Delphic shock increases the financial markets' appetite for risk and this pushes the dollar down, in practice roughly canceling any effect of higher US interest rates.

8 Conclusions

This paper exploits the high kurtosis of financial market responses to pin down four main dimensions of FOMC announcements, which can be naturally labeled as: standard monetary policy, Odyssean forward guidance, LSAP and Delphic forward guidance. These shocks have plausible effects on financial markets and provide intuitive interpretations of the FOMC announcements in the sample. The paper explains the intuition behind the fat tails-based identification and shows that it requires only a sufficient degree of independence, rather than full independence. It proposes estimation approaches that can be applied in many other applications.

Online Appendices

Appendix A Sensitivity of the results to the degree of non-Gaussianity

This section studies to what extent the identification weakens as we impose a higher degree of freedom parameter v in the Student t distribution. The results remain very similar for values of v between 1 and 10. For $v > 10$ the identification becomes weaker and the point estimates begin to change. However, even values much smaller than 10 are strongly rejected in favor of the point estimate $v = 1.33$.

Figure A.1: Maximum log-likelihood conditional on different values of v

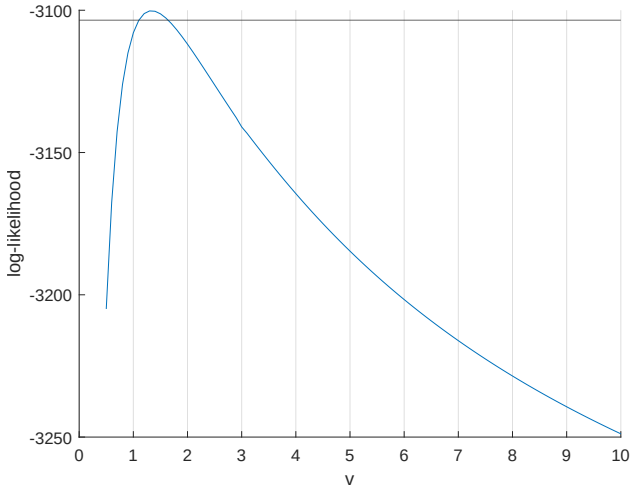

Note. The horizontal line shows the cut-off point implied by the likelihood ratio test at the 1% significance level.

To examine the sensitivity of the results to v I re-estimate model (4) fixing v at a grid of values from 0.5 to 30. Figure A.1 shows that the maximum attainable value of the log-likelihood decreases quickly as v deviates from the unconstrained estimate of 1.33. The figure is truncated at $v = 10$ for readability but the log-likelihood continues to decrease also for $v > 10$. The horizontal line at the top of the figure shows the cut-off point implied by the likelihood ratio test at the 1% significance level. We can see that already the null hypothesis

of $v = 2$ is rejected.

Figure A.2: The effects of standardized shocks, conditional on different values of v

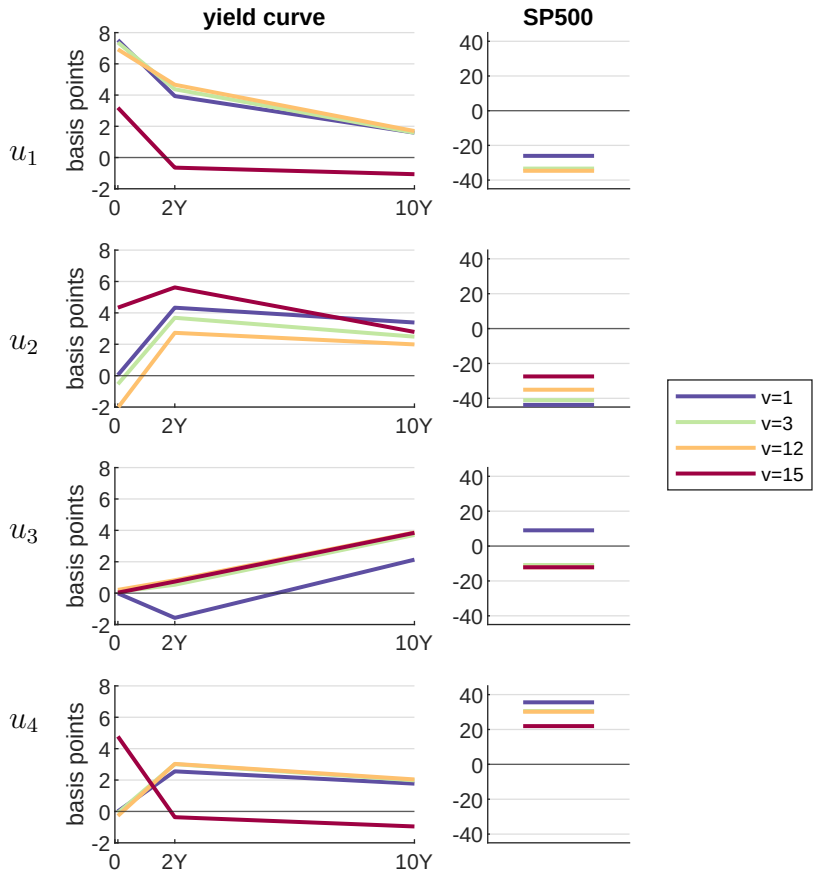

Figure A.2 shows that the effects of the four shocks are very similar for values of v from 1 to 12. Especially for the shocks u_1 and u_4 the estimates are difficult to distinguish in the figure as they lie almost on top of each other. The main visible difference is present for long-term rate shocks u_3: its effect on the 2-year yield is slightly negative for low v and becomes positive starting at about $v = 3$. The point estimates change qualitatively somewhere between $v = 12$ and $v = 15$: shocks u_1 and u_4 become essentially fed funds rate shocks with little effect on the longer maturities, while u_2 becomes an almost parallel shift of the whole yield curve including the shortest maturity. However, for $v = 15$ the uncertainty is substantially larger and many effects are no longer statistically significant (the same is true for $v = 12$, but not for $v \leq 10$).

Appendix B Additional figures

Figure B.1: The effects of selected FOMC announcements before 2008

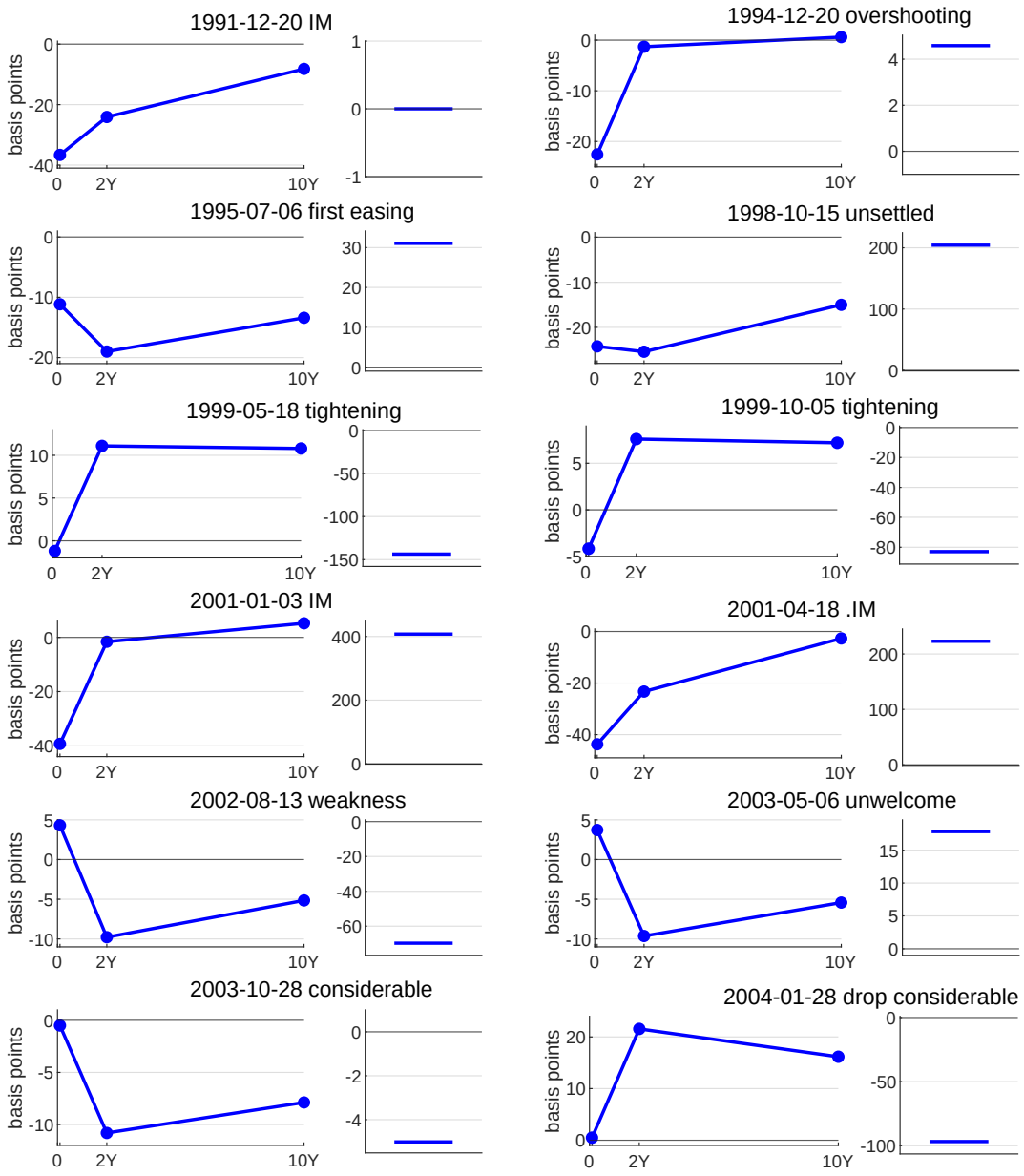

Note. The horizontal line in the right subplots represents the change of the S&P500 stock index. IM stands for an "inter-meeting" announcement.

Figure B.2: The effects of selected FOMC announcements since 2008

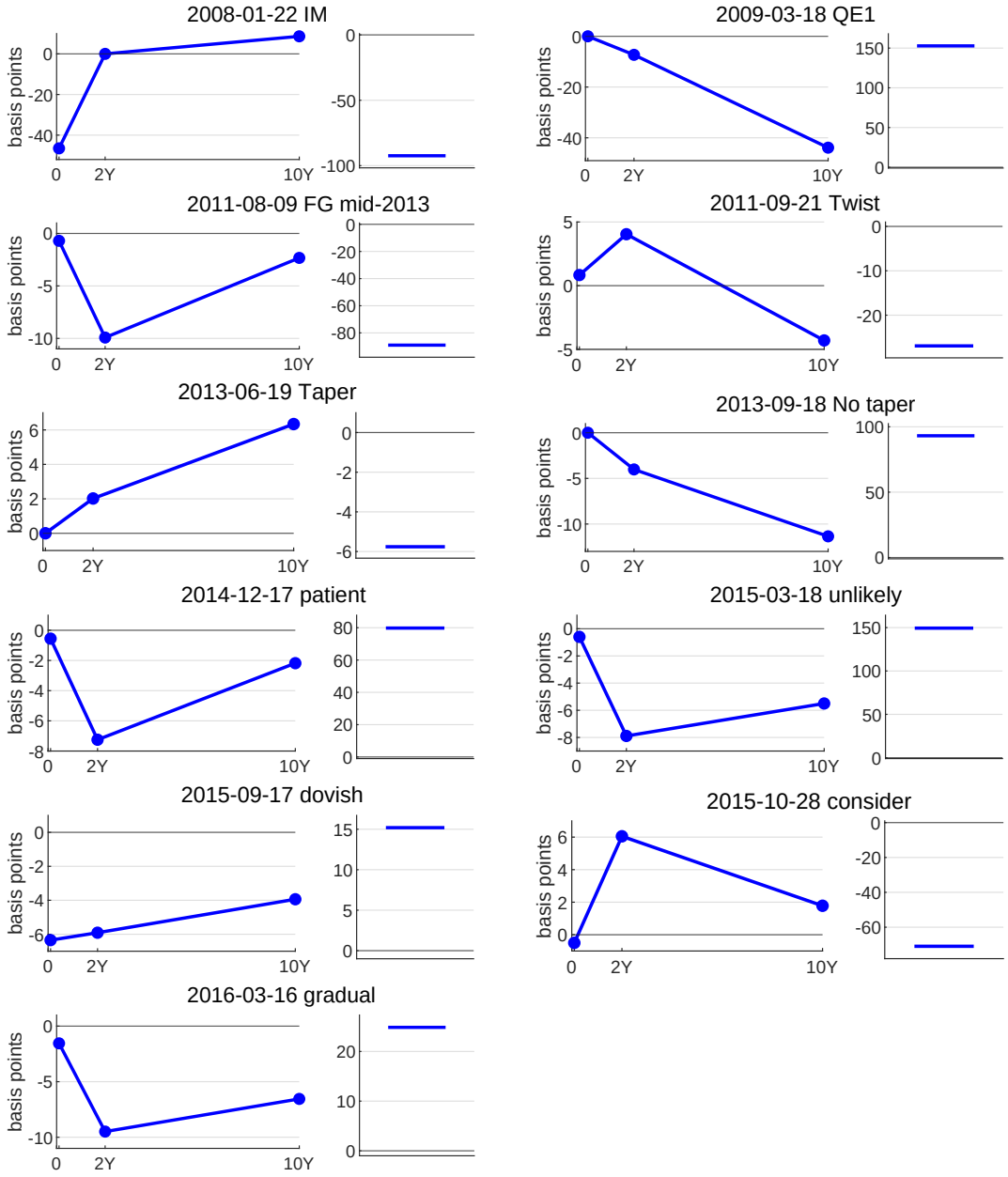

Note. The horizontal line in the right subplots represents the change of the S&P500 stock index.

Appendix C Analytical results used in the estimation

C.1 The gradient of the likelihood function in the baseline model

I derive the analytical gradient of the log-likelihood (4) with the help of the results in Magnus and Neudecker (2019) and Khatri and Rao (1968). Differentiating (4) w.r.t. $\operatorname{vec} W$ yields

$$\frac{d \log p(Y|W,v)}{d \operatorname{vec} W} = T \operatorname{vec} W^{-1\prime} + \iota_T'(A \bullet Y) \tag{C.1}$$

where $\bullet$ denotes the row-wise Khatri-Rao product,

$$A \bullet Y = \begin{pmatrix} a_1' \otimes y_1' \\ \dots \\ a_T \otimes y_T \end{pmatrix}, \tag{C.2}$$

a_t is an $N \times 1$ vector with the n-th element

$$a_{t,n} \equiv -\frac{v+1}{v} \frac{u_{t,n}}{1 + u_{t,n}^2/v}, \tag{C.3}$$

and ι_T denotes a $T \times 1$ vector with each element equal to 1.

Differentiating (4) w.r.t. v yields

$$\frac{d \log p(Y|W,v)}{dv} = -\frac{1}{2} \sum_t \sum_n \log(1 + u_{t,n}^2/v) + \frac{v+1}{2v^2} \sum_t \sum_n \frac{u_{t,n}^2}{(1 + u_{t,n}^2/v)} + TN \frac{d \log c(v)}{dv} \tag{C.4}$$

where

$$\frac{d \log c(v)}{dv} = -\frac{1}{2v} - \frac{1}{2}\psi(\tfrac{v}{2}) + \frac{1}{2}\psi(\tfrac{v+1}{2}) \tag{C.5}$$

where ψ denotes the digamma function (i.e. the derivative of the log of the Gamma function).

In practice, I reparameterize the log-likelihood in terms of $z = log(v)$.

C.2 The conditional posteriors of q_{nt}, v_n in the PDMT model

In the next two paragraphs I omit the subscript t to avoid clutter.

The conditional posterior of q_n, $n = 1, 2, ...N$ is

$$p(q_n|\cdot) \propto q_n^{v_n/2-1}(q_0 + q_n)^{1/2} \exp\left(-\frac{1}{2}\left(1 + \frac{u_n^2}{v_0 + v_n}\right) q_n\right) \tag{C.6}$$

This is a nonstandard density, which resembles the Gamma density except for the presence of the sum $(q_0 + q_n)$. Therefore, I draw q_n from the proposal Gamma density obtained by setting q_0 to zero and accept the proposal draw with the probability analogous to (18).

The conditional posterior of q_0 is

$$p(q_0|\cdot) \propto q_0^{v_0/2-1} \prod_{n=1}^{N}(q_0 + q_n)^{1/2} \exp\left(-\frac{1}{2} q_0 \left(1 + \sum_{n=1}^{N} \frac{u_n^2}{v_0 + v_n}\right)\right) \tag{C.7}$$

Again, this density resembles the Gamma density except for the presence of the sum (q_0+q_n) and as the proposal I use the Gamma density obtained by setting $q_n = 0$ for all n.

The conditional posterior of $\bar{v}$**:** Recall that $v_1 = ... = v_N = \bar{v}$. Let α_n, β_n denote the parameters of the Gamma prior for $\bar{v}$, with the kernel $\bar{v}^{\alpha_n - 1} \exp(-\bar{v}/\beta_n)$.

$$\begin{aligned} p(\bar{v}|\cdot) \propto{}& \bar{v}^{\alpha_n - 1} \exp(-\bar{v}/\beta_n) \Gamma(\bar{v}/2)^{-TN} 2^{-TN\bar{v}/2} \prod_{n=1}^{N}\prod_{t=1}^{T} q_{tn}^{\bar{v}/2} \\ &\times (v_0 + \bar{v})^{-TN/2} \exp\left(-\frac{1}{2(v_0 + \bar{v})} \sum_{n=1}^{N}\sum_{t=1}^{T} u_{tn}^2 (q_{t0} + q_{tn})\right) \end{aligned} \tag{C.8}$$

The conditional posterior of v_0: Let α_0, β_0 denote the parameters of the Gamma prior for v_0, with the kernel $\bar{v}^{\alpha_0 - 1} \exp(-\bar{v}/\beta_0)$.

$$p(v_0|\cdot) \propto v_0^{\alpha_0 - 1} \exp(-v_0/\beta_0) \Gamma(v_0/2)^{-T} 2^{-Tv_0/2} \prod_t^T q_{t0}^{v_0/2} \times \prod_n^N (v_0 + v_n)^{-T/2} \exp\left(-\frac{1}{2} \sum_n^N (v_0 + v_n)^{-1} \sum_t^T u_{tn}^2 (q_{t0} + q_{tn}) \right) \tag{C.9}$$

The conditional posteriors of $\bar{v}$ and v_0 are again nonstandard densities related to the Gamma density. To draw from them I follow Jiang and Ding (2016). I first compute the conditional posterior mode and the curvature at the mode. Then I find the Gamma density with the same mode and curvature at the mode and I use that Gamma density as the proposal density.

In an alternative simulation I also use the approach of matching the mode and the curvature at the mode to obtain proposal densities for $q_0, q_1, ..., q_N$. In this case the acceptance rates are lower but, with the 1 million-long chain, all estimation results are very similar and the simulation is substantially slower. This indicates that the simple Gamma proposal densities for q_n's are good enough in my case.

References

Avdjiev, Stefan, Wenxin Du, Cathérine Koch, and Hyun Song Shin (2019) "The Dollar, Bank Leverage, and Deviations from Covered Interest Parity," *American Economic Review: Insights*, 1 (2), 193–208, 10.1257/aeri.20180322.

Bauer, Michael D and Eric T Swanson (2022) "A Reassessment of Monetary Policy Surprises and High-Frequency Identification," Working Paper 29939, National Bureau of Economic Research, 10.3386/w29939.

Baumeister, Christiane and James D. Hamilton (2015) "Sign Restrictions, Structural Vector Autoregressions, and Useful Prior Information," *Econometrica*, 83 (5), 1963–1999, 10.3982/ecta12356.

Bernanke, Ben S. and Kenneth N. Kuttner (2005) "What Explains the Stock Market's Reaction to Federal Reserve Policy?" *The Journal of Finance*, 60 (3), 1221–1257, 10.1111/j.1540-6261.2005.00760.x.

Bonhomme, Stephane and Jean-Marc Robin (2009) "Consistent noisy independent component analysis," *Journal of Econometrics*, 149 (1), 12–25, 10.1016/j.jeconom.2008.12.019.

Braun, Robin (2021) "The importance of supply and demand for oil prices: evidence from non-Gaussianity,"Technical report, Bank of England.

Brunnermeier, Markus, Darius Palia, Karthik A. Sastry, and Christopher A. Sims (2021) "Feedbacks: Financial Markets and Economic Activity," *American Economic Review*, 111 (6), 1845–1879, 10.1257/aer.20180733.

Campbell, Jeffrey R., Charles L. Evans, Jonas D. M. Fisher, and Alejandro Justiniano (2012) "Macroeconomic Effects of Federal Reserve Forward Guidance," *Brookings Papers on Economic Activity*, 1–80, https://EconPapers.repec.org/RePEc:bin:bpeajo:v:43:y:2012:i:2012-01:p:1-80.

Cieślak, Anna and Andreas Schrimpf (2019) "Non-monetary news in central bank communication," *Journal of International Economics*, 118, 293–315, 10.1016/j.jinteco.2019.01.012.

Comon, Pierre (1994) "Independent component analysis, A new concept?" *Signal Processing*, 36 (3), 287 – 314, 10.1016/0165-1684(94)90029-9.

Davis, Richard and Serena Ng (2022) "Time Series Estimation of the Dynamic Effects of Disaster-Type Shock,"Technical Report arXiv:2107.06663v2, ArXiV, 10.48550/arXiv.2107.06663.

Del Negro, Marco, Marc Giannoni, and Christina Patterson (2012) "The forward guidance puzzle," Staff Reports 574, Federal Reserve Bank of New York, https://ideas.repec.org/p/fip/fednsr/574.html, Revised December 2015.

Drautzburg, Thorsten and Jonathan H. Wright (2021) "Refining Set-Identification in VARs through Independence," NBER Working Papers 29316, National Bureau of Economic Research, Inc, 10.3386/w29316.

Fiorentini, Gabriele and Enrique Sentana (2020) "Discrete Mixtures of Normals Pseudo Maximum Likelihood Estimators of Structural Vector Autoregressions," Working Papers wp2020-2023, CEMFI, https://ideas.repec.org/p/cmf/wpaper/wp2020_2023.html.

Geweke, John (1992) "Evaluating the Accuracy of Sampling-Based Approaches to the Calculation of Posterior Moments," in Berger, J.O., J.M. Bernardo, A.P. Dawid, and A.F.M. Smith eds. *Bayesian Statistics*, 169–193: Oxford University Press, Proceedings of the Fourth Valencia International Meeting on Bayesian Statistic.

Giacomini, Rafaella and Toru Kitagawa (2021) "Robust Bayesian inference for set-identified models," *Econometrica*, 89 (4), 1519–1556, 10.3982/ecta16773.

Gouriéroux, Christian, Alain Monfort, and Jean-Paul Renne (2017) "Statistical inference for independent component analysis: Application to structural VAR models," *Journal of Econometrics*, 196 (1), 111 – 126, https://doi.org/10.1016/j.jeconom.2016.09.007.

——— (2020) "Identification and Estimation in Non-Fundamental Structural VARMA Models," *The Review of Economic Studies*, 87 (4), 1915–1953, 10.1093/restud/rdz028.

Gürkaynak, Refet S., Hatice Gökçe Karasoy-Can, and Sang Seok Lee (forthcoming) "Stock Market's Assessment of Monetary Policy Transmission: The Cash Flow Effect," *Journal of Finance*.

Gürkaynak, Refet S., Brian Sack, and Eric Swanson (2005) "Do Actions Speak Louder Than Words? The Response of Asset Prices to Monetary Policy Actions and Statements," *International Journal of Central Banking*, 1 (1), 55–93, https://ideas.repec.org/a/ijc/ijcjou/y2005q2a2.html.

Hyvärinen, Aapo, Juha Karhunen, and Erkki Oja (2001) *Independent Component Analysis*: Wiley.

Inoue, Atsushi and Barbara Rossi (2018) "A new approach to measuring economic policy shocks, with an application to conventional and unconventional monetary policy," Economics Working Papers 1638, Department of Economics and Business, Universitat Pompeu Fabra, https://ideas.repec.org/p/upf/upfgen/1638.html.

Jacquier, Eric, Michael Johannes, and Nicholas Polson (2007) "MCMC maximum likelihood for latent state models," *Journal of Econometrics*, 137 (2), 615–640, 10.1016/j.jeconom.2005.11.017.

Jarociński, Marek and Peter Karadi (2020) "Deconstructing Monetary Policy Surprises - The Role of Information Shocks," *American Economic Journal: Macroeconomics*, 12 (2), 1–43, 10.1257/mac.20180090.

Jiang, Zhichao and Peng Ding (2016) "Robust modeling using non-elliptically contoured multivariate t distributions," *Journal of Statistical Planning and Inference*, 177, 50–63, 10.1016/j.jspi.2016.04.004.

Jones, M.C. (2002) "A dependent bivariate t distribution with marginals on different degrees of freedom," *Statistics & Probability Letters*, 56 (2), 163–170, 10.1016/S0167-7152(01)00180-8.

Khatri, C. G. and C. Radhakrishna Rao (1968) "Solutions to some functional equations and their applications to characterization of probability distributions," *Sankhya*, 30, 167–180.

Kuttner, Kenneth N. (2001) "Monetary Policy Surprises and Interest Rates: Evidence from the Fed Funds Futures Market," *Journal of Monetary Economics*, 47 (3), 523–544, 10.1016/S0304-3932(01)00055-1.

Lanne, Markku, Mika Meitz, and Pentti Saikkonen (2017) "Identification and estimation of non-Gaussian structural vector autoregressions," *Journal of Econometrics*, 196 (2), 288 – 304, 10.1016/j.jeconom.2016.06.002.

Lewis, Daniel J. (2019) "Announcement-Specific Decompositions of Unconventional Monetary Policy Shocks and Their Macroeconomic Effects," Staff Reports 891, Federal Reserve Bank of New York, https://ideas.repec.org/p/fip/fednsr/891.html.

Lewis, Daniel J (2021) "Identifying Shocks via Time-Varying Volatility," *The Review of Economic Studies*, 88 (6), 3086–3124, 10.1093/restud/rdab009.

Lewis, Daniel J. (forthcoming) "Robust Inference in Models Identified via Heteroskedasticity," *Review of Economics and Statistics*.

Magnus, Jan R. and Heinz Neudecker (2019) *Matrix Differential Calculus with Applications in Statistics and Econometrics*: John Wiley, 3rd edition, 10.1002/9781119541219.

Melosi, Leonardo (2017) "Signalling Effects of Monetary Policy," *The Review of Economic Studies*, 84 (2), 853–884, 10.1093/restud/rdw050.

Miescu, Mirela (2021) "Forward guidance and conventional monetary policy shocks: identification and assessment," mimeo, Lancaster University.

Miranda-Agrippino, Silvia and Giovanni Ricco (2021) "The Transmission of Monetary Policy Shocks," *American Economic Journal: Macroeconomics*, 13 (3), 74–107, 10.1257/mac.20180124.

Montiel Olea, José Luis, Mikkel Plagborg-Møller, and Eric Qian (2022) "SVAR Identification From Higher Moments: Has the Simultaneous Causality Problem Been Solved?", Prepared for AEA Papers and Proceedings.

Nakamura, Emi and Jón Steinsson (2018) "High-Frequency Identification of Monetary Non-Neutrality: The Information Effect," *The Quarterly Journal of Economics*, 133 (3), 1283–1330, 10.1093/qje/qjy004.

Rigobon, Roberto (2003) "Identification Through Heteroskedasticity," *The Review of Economics and Statistics*, 85 (4), 777–792, 10.1162/003465303772815727.

Shaw, William T. and K.T.A. Lee (2008) "Bivariate Student t distributions with variable marginal degrees of freedom and independence," *Journal of Multivariate Analysis*, 99 (6), 1276 – 1287, 10.1016/j.jmva.2007.08.006.

Sims, Christopher A. (2021) "SVAR Identification through Heteroskedasticity with Misspecified Regimes,"Technical report, Princeton University, http://sims.princeton.edu/yftp/bpss/IDHmsspcfdRgms.pdf.

Swanson, Eric T. (2021) "Measuring the Effects of Federal Reserve Forward Guidance and Asset Purchases on Financial Markets," *Journal of Monetary Economics*, 118, 32–53, 10.1016/j.jmoneco.2020.09.003.

Van Nieuwerburgh, Stijn and Laura Veldkamp (2010) "Information Acquisition and Under-Diversification," *Review of Economic Studies*, 77 (2), 779–805, 10.1111/j.1467-937X.2009.00583.x.

Waggoner, Daniel F. and Tao Zha (2003) "Likelihood preserving normalization in multiple equation models," *Journal of Econometrics*, 114 (2), 329–347, 10.1016/S0304-4076(03)00087-3.